Journal of Applied Analysis and Computation
Volume 11, Number 4, August 2021, 1982–2016
Website:http://www.jaac-online.com
DOI:10.11948/20200302

A TWO-PATCH MODEL FOR THE COVID-19 TRANSMISSION DYNAMICS IN CHINA*

Jie Bai[1,†] and Jin Wang[2]

Abstract In this paper, we study the COVID-19 epidemic in China and investigate its transmission dynamics. We propose a two-patch model in a spatially heterogeneous setting that incorporates multiple transmission pathways. We focus our attention on the roles of the environmental reservoir and the spatial heterogeneity in shaping the overall epidemic pattern. We conduct a detailed analysis on the global dynamics of the model, and demonstrate the application of our model through the incorporation of realistic data.

Keywords Compartmental modeling, basic reproduction number, equilibrium analysis

MSC(2010) 34A34, 37N25.

1. Introduction

The Coronavirus Disease 2019 (COVID-19) is caused by a novel coronavirus named severe acute respiratory syndrome coronavirus 2 (SARS-CoV-2). This virus is regarded as the third zoonotic human coronavirus emerging in the current century, after SARS-CoV in 2002 and the Middle East respiratory syndrome coronavirus (MERS-CoV) in 2012. On March 11, 2020, the World Health Organization (WHO) declared COVID-19 as a global pandemic. With over 20 million cases reported in more than 210 countries and territories as of August 10, 2020, COVID-19 has triggered unprecedented crises in public health and the economy throughout the world.

In order to better understand the transmission dynamics of COVID-19 and to design more effective disease control strategies, a number of mathematical and computational models have been proposed (see, e.g., [5, 6, 8–12]). Almost all these models are based on the susceptible-exposed-infected-recovered (SEIR) compartmental framework or its variants, focused on the human-to-human direct transmission pathway [1, 15]. On the other hand, the indirect transmission pathway from the environment to human hosts is also a highly possible route to spread the coronavirus, but has not been adequately investigated in current modeling studies. When infected individuals cough or sneeze, they release the coronavirus through

†The corresponding author. Email: linlanfaith@aliyun.com(J. Bai)
1School of Mathematics, Liaoning University, Chongshan Middle Road 66, 110036 Shenyang, China
2Department of Mathematics, University of Tennessee at Chattanooga, Chattanooga, TN 37403, USA
*The first author was supported by Natural Science Youth Project of The Educational Department of Liaoning Province (LQN202004) and Youth Research Fund Project of Liaoning University (2012LDQN02).

their respiratory droplets. Most of these droplets would fall on nearby surfaces and objects, and other individuals could catch the virus by touching the contaminated surfaces or objects. Meanwhile, some of the coronaviruses released by infected individuals could float in the air as aerosols which can be breathed in by other people. A recent experimental study found that SARS-CoV-2 was detectable in aerosols for up to 3 hours, on copper for up to 4 hours, on cardboard for up to 24 hours, and on plastic and stainless steel for up to 3 days [3]. The fact that this virus can remain viable in aerosols and on surfaces for an extended period of time indicate a risk of environmental transmission, particularly airborne and fomite transmission, for SARS-CoV-2. Additionally, the novel coronavirus has been found in the stool of some infected individuals [4], which may contaminate the aquatic environment through the sewage water and could add another possible route of environmental transmission for COVID-19 [14].

Another limitation in the current COVID-19 models is the insufficient understanding of the spatial heterogeneity in the transmission and spread of the disease. Different population characteristics, mobility patterns and environmental conditions could lead to highly varied disease prevalence and incidence. For example, COVID-19 started in China in December 2019, and the city of Wuhan became the first epicenter; at the province level, cases reported in Hubei province, which Wuhan city belongs to, account for more than 80% of the total cases reported in the entire country of China. For another example, among the 50 states and several territories of the US that reported COVID-19 infections, the 4 states of California, Florida, New York and Texas represent more than 40% of the total cases. These data suggest that the underlying transmission rates, infection risks and disease burdens vary from place to place. Many factors lead to such variations. In particular, the movement of human hosts and the different environmental distributions of SARS-CoV-2 could increase the degree of spatial heterogeneity and contribute to the complex pattern of the COVID-19 pandemic.

In the present study, we aim to partially fill the knowledge gap related to the two aforementioned challenges in COVID-19 modeling, by proposing and studying a two-patch model in a spatially heterogeneous setting that incorporates multiple transmission pathways. We focus our attention on the country of China, where COVID-19 was first reported, and consider the period from January to February in 2020, when the disease outbreak was most severe in China. We emphasize the role of the environmental reservoirs in our model. The environmental reservoirs here, defined in a broad sense, include the air, water, and all surfaces and objects surrounding human individuals. We consider both the human-to-human and environment-to-human transmission routes, coupled with different spatial characteristics in a two-patch setting. The motivations for this study are threefold: (1) to better understand the spatial dynamics of COVID-19; (2) to gain more knowledge on the role of the environmental reservoirs in the transmission of COVID-19; and (3) to investigate how the multiple transmission pathways and spatial heterogeneity are coupled together to shape the overall pattern of the disease dynamics.

The remainder of this paper is organized as follows. In Section 2, we present the formulation of our mathematical model. In Sections 3 and 4, we conduct a detailed analysis for this model and establish its threshold type dynamics. In Section 5, we conduct numerical simulation and fit our model to the publicly reported data in China. In Section 6, we conclude the paper with some discussion.

2. Model formulation

Given the different incidence and prevalence levels of COVID-19 in China, we divide the entire country into two patches: patch 1 for Hubei province, and patch 2 for the remaining part of China. Within each patch, we divide the total human population into four compartments: the susceptible (denoted by S), the exposed (denoted by E), and the infected (denoted by I). Individuals in the infected class have fully developed disease symptoms and can infect other people. Individuals in the exposed class are in the incubation period; they do not show symptoms but are still capable of infecting others. Meanwhile, to study the role of the environmental reservoirs in the transmission of this disease, we introduce V to denote the concentration of the coronavirus in the environment. We describe the COVID-19 transmission dynamics by the following system.

Patch 1:

$$\begin{aligned}
\frac{dS_1}{dt} &= \Lambda_1 - \beta_{E_1} S_1 E_1 - \beta_{I_1} S_1 I_1 - \beta_{V_1} S_1 V_1 - \mu S_1 + a_2 S_2,\\
\frac{dE_1}{dt} &= \beta_{E_1} S_1 E_1 + \beta_{I_1} S_1 I_1 + \beta_{V_1} S_1 V_1 - (\alpha + \mu) E_1 + b_2 E_2,\\
\frac{dI_1}{dt} &= \alpha E_1 - (w_1 + \gamma + \mu) I_1,\\
\frac{dV_1}{dt} &= \xi E_1 - \sigma V_1.
\end{aligned} \tag{2.1}$$

Patch 2:

$$\begin{aligned}
\frac{dS_2}{dt} &= \Lambda_2 - \beta_{E_2} S_2 E_2 - \beta_{I_2} S_2 I_2 - \beta_{V_2} S_2 V_2 - \mu S_2 - a_2 S_2,\\
\frac{dE_2}{dt} &= \beta_{E_2} S_2 E_2 + \beta_{I_2} S_2 I_2 + \beta_{V_2} S_2 V_2 - (\alpha + \mu) E_2 - b_2 E_2,\\
\frac{dI_2}{dt} &= \alpha E_2 - (w_2 + \gamma + \mu) I_2,\\
\frac{dV_2}{dt} &= \xi E_2 - \sigma V_2.
\end{aligned} \tag{2.2}$$

The parameter μ is the natural death rate of human hosts in China, α^{-1} is the incubation period between the infection and the onset of symptoms, γ is the rate of recovery from infection, ξ is the rate of the exposed individuals contributing the coronavirus to the environmental reservoir, and σ is the removal rate of the virus from the environment. We assume that these rates are the same for both patches. We also assume that (symptomatic) infected individuals are strictly isolated and treated in the hospitals and so their contribution of the coronavirus to the environment can be neglected. The parameters β_{E_j} and β_{I_j} represent the direct, human-to-human transmission rates between the exposed and susceptible individuals, and between the infected and susceptible individuals, respectively, in patch j ($j = 1, 2$), and β_{V_j} represents the indirect, environment-to-human transmission rate in patch j ($j = 1, 2$). Meanwhile, we let Λ_1 and Λ_2 denote the population influx rates due to newborns, and w_1 and w_2 the disease-induced death rates, in patches 1 and 2, respectively. Additionally, due to the lockdown of all the major cities in Hubei province and the strict quarantine policy imposed by the Chinese government (starting from January 23, 2020), we assume that no human hosts can move from patch 1 to patch 2, while susceptible and exposed individuals move from patch 2 to patch 1 at rates a_2 and b_2, respectively.

3. Dynamics of patch 2

Our model consists of two subsystems (2.1) and (2.2). Clearly, (2.1) depends on (2.2), whereas (2.2) is independent of (2.1). Thus it is natural to start our analysis by examining the subsystem (2.2).

3.1. Reproduction number of patch 2

We first calculate the reproduction number $\mathcal{R}_{02}$ for patch 2. Obviously, the disease-free equilibrium (DFE) of patch 2 is

$$x_{20} = (S_{20}, 0, 0, 0) = \Big(\frac{\Lambda_2}{\mu + a_2}, 0, 0, 0\Big) \tag{3.1}$$

which is unique. Furthermore, the new infection matrix $\mathcal{F}$ and the transition matrix $\mathcal{V}$ are

$$\mathcal{F}_2 = \begin{pmatrix} \beta_{E_2} S_{20} & \beta_{I_2} S_{20} & \beta_{V_2} S_{20} \\ 0 & 0 & 0 \\ 0 & 0 & 0 \end{pmatrix},$$

and

$$\mathcal{V}_2 = \begin{pmatrix} \alpha + \mu + b_2 & 0 & 0 \\ -\alpha & \omega_2 + \gamma + \mu & 0 \\ -\xi & 0 & \sigma \end{pmatrix}.$$

Thus,

$$\mathcal{F}_2 \mathcal{V}_2^{-1} = \begin{pmatrix} \frac{\beta_{E_2} S_{20}}{\alpha+\mu+b_2} + \frac{\alpha\beta_{I_2} S_{20}}{(\alpha+\mu+b_2)(\omega_2+\gamma+\mu)} + \frac{\xi\beta_{V_2} S_{20}}{(\alpha+\mu+b_2)\sigma} & \frac{\beta_{I_2} S_{20}}{\omega_2+\gamma+\mu} & \frac{\beta_{V_2} S_{20}}{\sigma} \\ 0 & 0 & 0 \\ 0 & 0 & 0 \end{pmatrix}.$$

By the next-generation matrix method [2], the reproduction number is given by

$$\mathcal{R}_{02} = \rho(\mathcal{F}_2 \mathcal{V}_2^{-1}) = \frac{\beta_{E_2} S_{20}}{\alpha+\mu+b_2} + \frac{\alpha\beta_{I_2} S_{20}}{(\alpha+\mu+b_2)(\omega_2+\gamma+\mu)} + \frac{\xi\beta_{V_2} S_{20}}{(\alpha+\mu+b_2)\sigma}. \tag{3.2}$$

We observe that $\mathcal{R}_{02}$ consists of three parts, representing the contribution from the three respective transmission routes: exposed-to-susceptible direct transmission, infected-to-susceptible direct transmission, and environment-to-human indirect transmission. These three transmission modes collectively shape the infection risk of COVID-19 in patch 2.

3.2. Stability of equilibria in patch 2

We first state the following result.

Theorem 3.1. *For the subsystem (2.2), when $\mathcal{R}_{02} < 1$, there is only one equilibrium, the DFE, which is locally asymptotically stable; when $\mathcal{R}_{02} > 1$, in addition to the DFE, there is a unique endemic equilibrium.*

Proof. We only need to show the existence and uniqueness of the endemic equilibrium when $\mathcal{R}_{02} > 1$. Consider the following equations at the equilibrium:

$$\Lambda_2 - \beta_{E_2} S_2 E_2 - \beta_{I_2} S_2 I_2 - \beta_{V_2} S_2 V_2 - \mu S_2 - a_2 S_2 = 0, \tag{3.3}$$
$$\beta_{E_2} S_2 E_2 + \beta_{I_2} S_2 I_2 + \beta_{V_2} S_2 V_2 - (\alpha + \mu) E_2 - b_2 E_2 = 0, \tag{3.4}$$
$$\alpha E_2 - (w_2 + \gamma + \mu) I_2 = 0, \tag{3.5}$$
$$\xi E_2 - \sigma V_2 = 0. \tag{3.6}$$

Multiplying equation (3.4) with $w_2 + \gamma + \mu$ and equation (3.5) with $\beta_{I_2} S_2$, and adding the results, we obtain

$$E_2 \Big[\beta_{E_2} S_2 + \beta_{V_2} S_2 \cdot \frac{\xi}{\sigma} + \frac{\alpha \beta_{I_2} S_2}{w_2 + \gamma + \mu} - (\alpha + \mu + b_2) \Big] = 0. \tag{3.7}$$

Since $E_2 \neq 0$ at the endemic equilibrium, we can immediately solve for S_2 from equation (3.7). Then adding equations (3.3) and (3.4), we can solve for E_2, which subsequently determines I_2 and V_2 from equations (3.5) and (3.6). Hence, the endemic equilibrium in patch 2, if it exists, must be unique and given by

$$x_2^E = (S_2^E, E_2^E, I_2^E, V_2^E) \tag{3.8}$$

where $S_2^E = \frac{\alpha+\mu+b_2}{\beta_{E_2} + \beta_{V_2} \cdot \frac{\xi}{\sigma} + \frac{\alpha \beta_{I_2}}{w_2+\gamma+\mu}}$, $E_2^E = \frac{\Lambda_2 - (\mu + a_2) S_2^E}{\alpha+\mu+b_2}$, $I_2^E = \frac{\alpha E_2^E}{w_2+\gamma+\mu}$, and $V_2^E = \frac{\xi E_2^E}{\sigma}$. The existence of the endemic equilibrium requires $S_2^E, E_2^E, I_2^E, V_2^E > 0$, which is equivalent to $\mathcal{R}_{02} > 1$ through simple algebraic verification. □

Clearly, the DFE is locally asymptotically stable when $\mathcal{R}_{02} < 1$ and becomes unstable when $\mathcal{R}_{02} > 1$ [2]. A local stability analysis for the endemic equilibrium when $\mathcal{R}_{02} > 1$ is presented in Appendix A. Next, we conduct global stability analysis for the DFE and the endemic equilibrium. Define the domain

$$\begin{aligned} \Delta = &\big\{(S_2, E_2, I_2, V_2) : S_2, E_2, I_2, V_2 \geq 0, S_2 \leq S_{20}, \\ &S_2 + E_2 + I_2 \leq \Lambda_2/\mu, V_2 \leq \xi \Lambda_2/(\mu\sigma)\big\}. \end{aligned}$$

It is clear that Δ is positively invariant for the subsystem (2.2). The following theorem summarizes the global stability results.

Theorem 3.2. *(1) When $\mathcal{R}_{02} < 1$, the disease-free equilibrium of subsystem (2.2) is globally asymptotically stable in Δ. (2) When $\mathcal{R}_{02} > 1$, the endemic equilibrium of subsystem (2.2) is globally asymptotically stable in the interior of Δ.*

Proof. (1) **Global stability of the DFE.** The subsystem (2.2) implies

$$\begin{aligned} \frac{dE_2}{dt} &\leq \beta_{E_2} S_{20} E_2 + \beta_{I_2} S_{20} I_2 + \beta_{V_2} S_{20} V_2 - (\alpha + \mu) E_2 - b_2 E_2, \\ \frac{dI_2}{dt} &\leq \alpha E_2 - (w_2 + \gamma + \mu) I_2, \end{aligned}$$

$$\frac{dV_2}{dt} \leq \xi E_2 - \sigma V_2. \tag{3.9}$$

Let $Y = (E_2, I_2, V_2)^T$. We then have

$$\frac{dY}{dt} \leq (\mathcal{F}_2 - \mathcal{V}_2)Y. \tag{3.10}$$

By the Perron-Frobenius theorem, there exists a non-negative left eigenvector u of the non-negative matrix $\mathcal{V}_2^{-1}\mathcal{F}_2$ with respect to the eigenvalue $\mathcal{R}_{02} = \rho(\mathcal{F}_2\mathcal{V}_2^{-1}) = \rho(\mathcal{V}_2^{-1}\mathcal{F}_2)$. We define the Lyapunov function:

$$L = u^T \mathcal{V}_2^{-1} Y.$$

Differentiating L along solutions of (2.2) implies

$$L' = u^T \mathcal{V}_2^{-1} \frac{dY}{dt} \leq u^T \mathcal{V}_2^{-1}(\mathcal{F}_2 - \mathcal{V}_2)Y = (\mathcal{R}_{02} - 1)u^T Y.$$

If $\mathcal{R}_{02} < 1$, then $L' \leq 0$, and $L' = 0$ leads to $u^T Y = 0$. Therefore, at least one of the three equations $E_2 = 0$, $I_2 = 0$ and $V_2 = 0$ must hold. By one of the three equations, we can obtain that the other two equations also hold based on subsystem (2.2). Thus, $E_2 = I_2 = V_2 = 0$. Consequently, $S_2 = S_{20}$. Hence, the largest invariant set where $L' = 0$ is the DFE $(S_{20}, 0, 0, 0)$. By LaSalle's Invariance Principle, the DFE is globally asymptotically stable in Δ when $\mathcal{R}_{02} < 1$.

(2) **Global stability of the endemic equilibrium.** We introduce the following Lyapunov function:

$$\begin{aligned} L = & \int_{S_2^E}^{S_2} \frac{u - S_2^E}{u} du + \int_{E_2^E}^{E_2} \frac{u - E_2^E}{u} du + \frac{\beta_{I_2} S_2^E I_2^E}{\alpha E_2^E} \int_{I_2^E}^{I_2} \frac{u - I_2^E}{u} du \\ & + \frac{\beta_{V_2} S_2^E V_2^E}{\xi E_2^E} \int_{V_2^E}^{V_2} \frac{u - V_2^E}{u} du \\ & \geq 0. \end{aligned}$$

Meanwhile, the following equations hold:

$$\Lambda_2 - \beta_{E_2} S_2^E E_2^E - \beta_{I_2} S_2^E I_2^E - \beta_{V_2} S_2^E V_2^E - \mu S_2^E - a_2 S_2^E = 0, \tag{3.11}$$
$$\beta_{E_2} S_2^E E_2^E + \beta_{I_2} S_2^E I_2^E + \beta_{V_2} S_2^E V_2^E - (\alpha + \mu)E_2^E - b_2 E_2^E = 0, \tag{3.12}$$
$$\alpha E_2^E - (w_2 + \gamma + \mu)I_2^E = 0, \tag{3.13}$$
$$\xi E_2^E - \sigma V_2^E = 0. \tag{3.14}$$

Using equations (3.11)-(3.14), we calculate the derivative of L along the solution of subsystem (2.2):

$$\begin{aligned} L'|_{Patch2} = & (1 - \frac{S_2^E}{S_2})[\Lambda_2 - \beta_{E_2} S_2 E_2 - \beta_{I_2} S_2 I_2 - \beta_{V_2} S_2 V_2 - \mu S_2 - a_2 S_2 \\ & - (\Lambda_2 - \beta_{E_2} S_2^E E_2^E - \beta_{I_2} S_2^E I_2^E - \beta_{V_2} S_2^E V_2^E - \mu S_2^E - a_2 S_2^E)] \\ & \text{(denoted as } k_1) \\ & + (1 - \frac{E_2^E}{E_2})\{[\beta_{E_2} S_2 E_2 + \beta_{I_2} S_2 I_2 + \beta_{V_2} S_2 V_2 - (\alpha + \mu)E_2 - b_2 E_2] \end{aligned}$$

$$- [\beta_{E_2} S_2^E E_2^E + \beta_{I_2} S_2^E I_2^E + \beta_{V_2} S_2^E V_2^E - (\alpha+\mu)E_2^E - b_2 E_2^E]\}$$
$$\text{(denoted as } k_2)$$
$$+ \frac{\beta_{I_2} S_2^E I_2^E}{\alpha E_2^E}(1 - \frac{I_2^E}{I_2})\{[\alpha E_2 - (w_2+\gamma+\mu)I_2]$$
$$- [\alpha E_2^E - (w_2+\gamma+\mu)I_2^E]\} \quad \text{(denoted as } k_3)$$
$$+ \frac{\beta_{V_2} S_2^E V_2^E}{\xi E_2^E}(1 - \frac{V_2^E}{V_2})[\xi E_2 - \sigma V_2 - (\xi E_2^E - \sigma V_2^E)]$$
$$\text{(denoted as } k_4).$$

We arrange k_1, k_2, k_3, k_4 as follows:

$$\begin{aligned}
k_1 =& (\mu+a_2)S_2^E(2 - \frac{S_2}{S_2^E} - \frac{S_2^E}{S_2}) + \beta_{E_2}(1 - \frac{S_2^E}{S_2})(S_2^E E_2^E - S_2 E_2) \\
&+ \beta_{I_2}(1 - \frac{S_2^E}{S_2})(S_2^E I_2^E - S_2 I_2) + \beta_{V_2}(1 - \frac{S_2^E}{S_2})(S_2^E V_2^E - S_2 V_2) \\
=& (\mu+a_2)S_2^E(2 - \frac{S_2}{S_2^E} - \frac{S_2^E}{S_2}) \quad \spadesuit_0 \\
&+ \beta_{E_2}[S_2^E E_2^E - S_2 E_2 - \frac{(S_2^E)^2 E_2^E}{S_2} + S_2^E E_2] \ \spadesuit_1 \\
&+ \beta_{I_2}[S_2^E I_2^E - S_2 I_2 - \frac{(S_2^E)^2 I_2^E}{S_2} + S_2^E I_2] \quad \spadesuit_2 \\
&+ \beta_{V_2}[S_2^E V_2^E - S_2 V_2 - \frac{(S_2^E)^2 V_2^E}{S_2} + S_2^E V_2] \ \spadesuit_3, \\
k_2 =& (\alpha+\mu+b_2)E_2^E(2 - \frac{E_2}{E_2^E} - \frac{E_2^E}{E_2}) + \beta_{E_2}(1 - \frac{E_2^E}{E_2})(S_2 E_2 - S_2^E E_2^E) \\
&+ \beta_{I_2}(1 - \frac{E_2^E}{E_2})(S_2 I_2 - S_2^E I_2^E) + \beta_{V_2}(1 - \frac{E_2^E}{E_2})(S_2 V_2 - S_2^E V_2^E) \\
=& (\alpha+\mu+b_2)E_2^E(2 - \frac{E_2}{E_2^E} - \frac{E_2^E}{E_2}) \quad \clubsuit \\
&+ \beta_{E_2}[-S_2^E E_2^E + S_2 E_2 + \frac{S_2^E (E_2^E)^2}{E_2} - S_2 E_2^E] \quad \heartsuit_1 \\
&+ \beta_{I_2}[-S_2^E I_2^E + S_2 I_2 - \frac{E_2^E S_2 I_2}{E_2} + \frac{E_2^E S_2^E I_2^E}{E_2}] \quad \heartsuit_2 \\
&+ \beta_{V_2}[-S_2^E V_2^E + S_2 V_2 - \frac{E_2^E S_2 V_2}{E_2} + \frac{E_2^E S_2^E V_2^E}{E_2}] \quad \heartsuit_3, \\
k_3 =& \frac{\beta_{I_2} S_2^E I_2^E}{\alpha E_2^E}(\omega_2+\gamma+\mu)I_2^E(2 - \frac{I_2}{I_2^E} - \frac{I_2^E}{I_2}) \\
&+ \frac{\beta_{I_2} S_2^E I_2^E}{\alpha E_2^E}\alpha E_2^E(\frac{E_2}{E_2^E} - 1 - \frac{I_2^E E_2}{I_2 E_2^E} + \frac{I_2^E}{I_2}) \\
=& \beta_{I_2} S_2^E I_2^E(1 - \frac{I_2}{I_2^E} + \frac{E_2}{E_2^E} - \frac{I_2^E E_2}{I_2 E_2^E}) \quad \diamondsuit \quad \text{(on the basis of (3.13))},
\end{aligned}$$

and

$$\begin{aligned}
k_4 &= \frac{\beta_{V_2} S_2^E V_2^E}{\xi E_2^E} \sigma V_2^E \left(1 - \frac{V_2^E}{V_2}\right)\left(1 - \frac{V_2}{V_2^E}\right) + \frac{\beta_{V_2} S_2^E V_2^E}{\xi E_2^E} \xi E_2^E \left(1 - \frac{V_2^E}{V_2}\right)\left(\frac{E_2}{E_2^E} - 1\right) \\
&= \frac{\beta_{V_2} S_2^E V_2^E}{\xi E_2^E} \sigma V_2^E \left(2 - \frac{V_2^E}{V_2} - \frac{V_2}{V_2^E}\right) + \frac{\beta_{V_2} S_2^E V_2^E}{\xi E_2^E} \xi E_2^E \left(\frac{E_2}{E_2^E} - 1 - \frac{V_2^E E_2}{V_2 E_2^E} + \frac{V_2^E}{V_2}\right) \\
&= \beta_{V_2} S_2^E V_2^E \left(1 - \frac{V_2}{V_2^E} + \frac{E_2}{E_2^E} - \frac{V_2^E E_2}{V_2 E_2^E}\right) \ \sharp \quad \text{(according to (3.14))}.
\end{aligned}$$

We continue the algebraic manipulation for the above equations. First, we have

$$\begin{aligned}
\clubsuit &= (\beta_{E_2} S_2^E E_2^E + \beta_{I_2} S_2^E I_2^E + \beta_{V_2} S_2^E V_2^E)\left(2 - \frac{E_2}{E_2^E} - \frac{E_2^E}{E_2}\right) \quad \text{(due to (3.12))} \\
&= \beta_{E_2} S_2^E E_2^E \left(2 - \frac{E_2}{E_2^E} - \frac{E_2^E}{E_2}\right) \ \clubsuit_1 \\
&\quad + \beta_{I_2} S_2^E I_2^E \left(2 - \frac{E_2}{E_2^E} - \frac{E_2^E}{E_2}\right) \ \clubsuit_2 \\
&\quad + \beta_{V_2} S_2^E V_2^E \left(2 - \frac{E_2}{E_2^E} - \frac{E_2^E}{E_2}\right) \ \clubsuit_3.
\end{aligned}$$

Second, we merge the same items:

$$\begin{aligned}
\clubsuit_1 + \spadesuit_1 + \heartsuit_1 &= \beta_{E_2} S_2^E E_2^E \left(2 - \frac{E_2}{E_2^E} - \frac{E_2^E}{E_2} + \frac{E_2}{E_2^E} - \frac{S_2^E}{S_2} + \frac{E_2^E}{E_2} - \frac{S_2}{S_2^E}\right) \\
&= \beta_{E_2} S_2^E E_2^E \left(2 - \frac{S_2}{S_2^E} - \frac{S_2^E}{S_2}\right), \\
\clubsuit_2 + \spadesuit_2 + \heartsuit_2 + \diamondsuit &= \beta_{I_2} S_2^E I_2^E \left(2 - \frac{E_2}{E_2^E} - \frac{E_2^E}{E_2} + 1 + \frac{E_2}{E_2^E} + \frac{E_2^E}{E_2} - \frac{I_2^E E_2}{I_2 E_2^E} \right.\\
&\qquad \left. - \frac{S_2^E}{S_2} - \frac{E_2^E S_2 I_2}{E_2 S_2^E I_2^E}\right) \\
&= \beta_{I_2} S_2^E I_2^E \left(3 - \frac{I_2^E E_2}{I_2 E_2^E} - \frac{S_2^E}{S_2} - \frac{E_2^E S_2 I_2}{E_2 S_2^E I_2^E}\right),
\end{aligned}$$

and

$$\begin{aligned}
\clubsuit_3 + \spadesuit_3 + \heartsuit_3 + \sharp &= \beta_{V_2} S_2^E V_2^E \left(2 - \frac{E_2}{E_2^E} - \frac{E_2^E}{E_2} + 1 + \frac{E_2}{E_2^E} + \frac{E_2^E}{E_2} - \frac{V_2^E E_2}{V_2 E_2^E} \right.\\
&\qquad \left. - \frac{S_2^E}{S_2} - \frac{E_2^E S_2 V_2}{E_2 S_2^E V_2^E}\right) \\
&= \beta_{V_2} S_2^E V_2^E \left(3 - \frac{V_2^E E_2}{V_2 E_2^E} - \frac{S_2^E}{S_2} - \frac{E_2^E S_2 V_2}{E_2 S_2^E V_2^E}\right).
\end{aligned}$$

Finally, adding the three equations above to the expression of $\spadesuit_0$, we conclude

$$\begin{aligned}
L'|_{Patch\,2} &= (\mu + a_2) S_2^E \left(2 - \frac{S_2}{S_2^E} - \frac{S_2^E}{S_2}\right) + \beta_{E_2} S_2^E E_2^E \left(2 - \frac{S_2}{S_2^E} - \frac{S_2^E}{S_2}\right) \\
&\quad + \beta_{I_2} S_2^E I_2^E \left(3 - \frac{I_2^E E_2}{I_2 E_2^E} - \frac{S_2^E}{S_2} - \frac{E_2^E S_2 I_2}{E_2 S_2^E I_2^E}\right)
\end{aligned}$$

$$+\beta_{V_2} S_2^E V_2^E \Big(3 - \frac{V_2^E E_2}{V_2 E_2^E} - \frac{S_2^E}{S_2} - \frac{E_2^E S_2 V_2}{E_2 S_2^E V_2^E}\Big)$$
$$\leq 0.$$

It is clear that

$$\{L'|_{Patch\,2} = 0\} = \{S_2 = S_2^E, E_2 = E_2^E, I_2 = I_2^E, V_2 = V_2^E\}.$$

Hence, according to LaSalle's Invariance Principle, the endemic equilibrium $x_2^E = (S_2^E, E_2^E, I_2^E, V_2^E)$ is globally asymptotically stable. □

4. Dynamics of the entire system

We have resolved the main dynamical properties of the single-patch subsystem (2.2), and Theorem 3.2 establishes the condition $\mathcal{R}_{02} = 1$ as a sharp threshold for disease extinction and disease persistence in patch 2. Now we proceed to analyze the coupled two-patch system (2.1) and (2.2).

4.1. Basic reproduction number of the entire system

Clearly the DFE of the two-patch system is unique and given by

$$x_0 = (S_{10}^*, E_{10}^*, I_{10}^*, V_{10}^*, S_{20}^*, E_{20}^*, I_{20}^*, V_{20}^*), \tag{4.1}$$

where $(S_{10}^*, E_{10}^*, I_{10}^*, V_{10}^*, S_{20}^*, E_{20}^*, I_{20}^*, V_{20}^*) = \Big(\frac{\Lambda_1 + \frac{\Lambda_2 a_2}{\mu + a_2}}{\mu}, 0, 0, 0, \frac{\Lambda_2}{\mu + a_2}, 0, 0, 0\Big)$.

The new infection matrix $\mathcal{F}$ and the transition matrix $\mathcal{V}$ are

$$\mathcal{F} = \begin{pmatrix} \beta_{E_1} S_{10}^* & \beta_{I_1} S_{10}^* & \beta_{V_1} S_{10}^* & b_2 & 0 & 0 \\ 0 & 0 & 0 & 0 & 0 & 0 \\ 0 & 0 & 0 & 0 & 0 & 0 \\ 0 & 0 & 0 & \beta_{E_2} S_{20}^* & \beta_{I_2} S_{20}^* & \beta_{V_2} S_{20}^* \\ 0 & 0 & 0 & 0 & 0 & 0 \\ 0 & 0 & 0 & 0 & 0 & 0 \end{pmatrix},$$

and

$$\mathcal{V} = \begin{pmatrix} \alpha + \mu & 0 & 0 & 0 & 0 & 0 \\ -\alpha & \omega_1 + \gamma + \mu & 0 & 0 & 0 & 0 \\ -\xi & 0 & \sigma & 0 & 0 & 0 \\ 0 & 0 & 0 & \alpha + \mu + b_2 & 0 & 0 \\ 0 & 0 & 0 & -\alpha & \omega_2 + \gamma + \mu & 0 \\ 0 & 0 & 0 & -\xi & 0 & \sigma \end{pmatrix}.$$

The next-generation matrix is

$$\mathcal{F}\mathcal{V}^{-1} = \begin{pmatrix} m_{11} & m_{12} & m_{13} & m_{14} & 0 & 0 \\ 0 & 0 & 0 & 0 & 0 & 0 \\ 0 & 0 & 0 & 0 & 0 & 0 \\ 0 & 0 & 0 & m_{44} & m_{45} & m_{46} \\ 0 & 0 & 0 & 0 & 0 & 0 \\ 0 & 0 & 0 & 0 & 0 & 0 \end{pmatrix},$$

where $m_{11} = \frac{\beta_{E_1} S_{10}^*}{\alpha+\mu} + \frac{\alpha\beta_{I_1} S_{10}^*}{(\alpha+\mu)(\omega_1+\gamma+\mu)} + \frac{\xi\beta_{V_1} S_{10}^*}{(\alpha+\mu)\sigma}$, $m_{12} = \frac{\beta_{I_1} S_{10}^*}{\omega_1+\gamma+\mu}$, $m_{13} = \frac{\beta_{V_1} S_{10}^*}{\sigma}$, $m_{14} = \frac{b_2}{\alpha+\mu+b_2}$, $m_{44} = \frac{\beta_{E_2} S_{20}^*}{\alpha+\mu+b_2} + \frac{\alpha\beta_{I_2} S_{20}^*}{(\alpha+\mu+b_2)(\omega_2+\gamma+\mu)} + \frac{\xi\beta_{V_2} S_{20}^*}{(\alpha+\mu+b_2)\sigma}$, $m_{45} = \frac{\beta_{I_2} S_{20}^*}{\omega_2+\gamma+\mu}$, $m_{46} = \frac{\beta_{V_2} S_{20}^*}{\sigma}$. Hence the basic reproduction number is given by

$$\mathcal{R}_0 = \rho(\mathcal{F}\mathcal{V}^{-1}) = \max\{\mathcal{R}_{01}, \mathcal{R}_{02}\}, \tag{4.2}$$

where

$$\mathcal{R}_{01} = \frac{S_{10}^*}{\alpha+\mu}\Big(\beta_{E_1} + \frac{\alpha\beta_{I_1}}{\omega_1+\gamma+\mu} + \frac{\xi\beta_{V_1}}{\sigma}\Big),\ \mathcal{R}_{02} = \frac{S_{20}^*}{\alpha+\mu+b_2}\Big(\beta_{E_2} + \frac{\alpha\beta_{I_2}}{\omega_2+\gamma+\mu} + \frac{\xi\beta_{V_2}}{\sigma}\Big). \tag{4.3}$$

The two terms $\mathcal{R}_{01}$ and $\mathcal{R}_{02}$ are the reproduction numbers for patches 1 and 2, respectively. Note that $\mathcal{R}_{02}$ is the same as defined in equation (3.2). $\mathcal{R}_{01}$, similar to $\mathcal{R}_{02}$, consists of three parts that represent the contributions from the three different transmission modes. Particularly, we emphasize the environment-to-human transmission component (i.e., the third component) in each of these two reproduction numbers, and we denote

$$\mathcal{R}_{01}^{EH} = \frac{S_{10}^*}{\alpha+\mu} \cdot \frac{\xi\beta_{V_1}}{\sigma}, \qquad \mathcal{R}_{02}^{EH} = \frac{S_{20}^*}{\alpha+\mu+b_2} \cdot \frac{\xi\beta_{V_2}}{\sigma}.$$

In addition, note that $\mathcal{R}_{01}$ depends on information from patch 2 due to the population movement. The maximum of $\mathcal{R}_{01}$ and $\mathcal{R}_{02}$ determines the overall infection risk of the entire system.

4.2. Stability of equilibria in the entire system

Through simple algebraic manipulation, we obtain that there are at most three biologically feasible equilibria for the coupled system (2.1) and (2.2): the DFE x_0 defined in equation (4.1), a boundary equilibrium

$$x^E = (S_1^E, E_1^E, I_1^E, V_1^E, S_{20}, 0, 0, 0), \tag{4.4}$$

and an endemic equilibrium

$$x^{EE} = (S_1^{EE}, E_1^{EE}, I_1^{EE}, V_1^{EE}, S_2^E, E_2^E, I_2^E, V_2^E) \tag{4.5}$$

where $(S_2^E, E_2^E, I_2^E, V_2^E)$ is the unique endemic equilibrium for the single-patch subsystem (2.2).

Below we analyze the dynamical behavior for each of these three equilibria. Define the domain

$$\begin{aligned}\Delta_E = &\Big\{(S_1, E_1, I_1, V_1, S_2, E_2, I_2, V_2) \geq 0 \,\Big|\, S_1 \leq S_{10}^*, S_2 \leq S_{20}^*; S_j + E_j + I_j \leq N_j,\\ &V_j \leq M_j, \text{for } j = 1, 2\Big\}\end{aligned}$$

where $N_1 = S_{10}^* + b_2\Lambda_2/\mu^2$, $N_2 = \Lambda_2/\mu$, $M_1 = \xi N_1/\sigma$, and $M_2 = \xi N_2/\sigma$. The upper bound in patch 1, N_1, is obtained by adding up the first three equations in system (2.1) and using the fact that $S_2 \leq N_2$ and $E_2 \leq N_2$. It is easy to observe that Δ_E is positively invariant for the system (2.1) and (2.2).

Theorem 4.1. *When $\mathcal{R}_{01} < 1$ and $\mathcal{R}_{02} < 1$ (i.e., $\mathcal{R}_0 < 1$), the DFE x_0 is the only equilibrium of the entire system and it is globally asymptotically stable in Δ_E.*

Proof. From system (2.1) and (2.2), we have

$$\begin{aligned}
\frac{dE_1}{dt} &\leq \beta_{E_1} S_{10}^* E_1 + \beta_{I_1} S_{10}^* I_1 + \beta_{V_1} S_{10}^* V_1 - (\alpha + \mu)E_1 + b_2 E_2,\\
\frac{dI_1}{dt} &\leq \alpha E_1 - (w_1 + \gamma + \mu)I_1,\\
\frac{dV_1}{dt} &\leq \xi E_1 - \sigma V_1,\\
\frac{dE_2}{dt} &\leq \beta_{E_2} S_{20}^* E_2 + \beta_{I_2} S_{20}^* I_2 + \beta_{V_2} S_{20}^* V_2 - (\alpha + \mu)E_2 - b_2 E_2,\\
\frac{dI_2}{dt} &\leq \alpha E_2 - (w_2 + \gamma + \mu)I_2,\\
\frac{dV_2}{dt} &\leq \xi E_2 - \sigma V_2.
\end{aligned}$$

Let $Z = (E_1, I_1, V_1, E_2, I_2, V_2)^T$. The inequalities above yield

$$\frac{dZ}{dt} \leq (\mathcal{F} - \mathcal{V})Z.$$

By the Perron-Frobenius theorem, there exists a non-negative left eigenvector v of the non-negative matrix $\mathcal{V}^{-1}\mathcal{F}$ with respect to the eigenvalue $\mathcal{R}_0 = \rho(\mathcal{F}\mathcal{V}^{-1}) = \rho(\mathcal{V}^{-1}\mathcal{F})$. We define the Lyapunov function:

$$L = v^T \mathcal{V}^{-1} Y.$$

Differentiating L along solutions of the system implies

$$L' = v^T \mathcal{V}^{-1} \frac{dZ}{dt} \leq v^T \mathcal{V}^{-1}(\mathcal{F} - \mathcal{V})Z = (\mathcal{R}_0 - 1)v^T Z.$$

If $\mathcal{R}_0 < 1$, then $L' \leq 0$. Using a similar argument as in the proof of Theorem 3.2, we can show that the largest invariant set where $L' = 0$ is the singleton $x_0 = (S_{10}^*, 0, 0, 0, S_{20}^*, 0, 0, 0)$. By LaSalle's Invariance Principle, the DFE is globally asymptotically stable when $\mathcal{R}_0 < 1$. □

Theorem 4.2. *When $\mathcal{R}_{01} > 1$ and $\mathcal{R}_{02} < 1$, the DFE x_0 and the boundary equilibrium x^E are the only equilibria of the two-patch system; furthermore, x_0 is unstable, and x^E is globally asymptotically stable.*

Proof. Since $\mathcal{R}_0 > 1$, the DFE x_0 is unstable [2]. Since $\mathcal{R}_{02} < 1$, the only equilibrium of the single-patch subsystem (2.2) is $x_{20} = (S_{20}, 0, 0, 0)$ based on Theorem 3.1. Through direct calculation, we can easily verify that in addition to x_0, the only equilibrium of the two-patch system is $x^E = (S_1^E, E_1^E, I_1^E, V_1^E, S_{20}, 0, 0, 0)$, where $S_1^E = \frac{\alpha+\mu}{\beta_{E_1}+\beta_{V_1}\cdot\frac{\xi}{\sigma}+\frac{\alpha\beta_{I_1}}{w_1+\gamma+\mu}}$, $E_1^E = \frac{\Lambda_1-\mu S_1^E+a_2S_{20}}{\alpha+\mu}$, $I_1^E = \frac{\alpha E_1^E}{\omega_1+\gamma+\mu}$, $V_1^E = \frac{\xi E_1^E}{\sigma}$. It is straightforward to observe that $S_1^E > 0$, and E_1^E, I_1^E, $V_1^E > 0$ if and only if $\mathcal{R}_{01} > 1$.

Next, we prove the global asymptotic stability of x^E. Since $\mathcal{R}_{02} < 1$, Theorem 3.2 states that $x_{20} = (S_{20}, 0, 0, 0)$ is globally asymptotically stable for the single-patch subsystem (2.2). Thus, $\lim_{t\to\infty} S_2(t) = S_{20}$, $\lim_{t\to\infty} E_2(t) = 0$, and it then suffices to consider the limiting system of (2.1):

$$\begin{aligned}
\frac{dS_1}{dt} &= \Lambda_1 - \beta_{E_1}S_1E_1 - \beta_{I_1}S_1I_1 - \beta_{V_1}S_1V_1 - \mu S_1 + a_2S_{20},\\
\frac{dE_1}{dt} &= \beta_{E_1}S_1E_1 + \beta_{I_1}S_1I_1 + \beta_{V_1}S_1V_1 - (\alpha+\mu)E_1,\\
\frac{dI_1}{dt} &= \alpha E_1 - (w_1+\gamma+\mu)I_1,\\
\frac{dV_1}{dt} &= \xi E_1 - \sigma V_1.
\end{aligned} \tag{4.6}$$

When $\mathcal{R}_{01} > 1$, system (4.6) admits a unique positive equilibrium (S_1^E, E_1^E, I_1^E, V_1^E). Specifically, we have the following equations:

$$\begin{aligned}
&\Lambda_1 - \beta_{E_1}S_1^EE_1^E - \beta_{I_1}S_1^EI_1^E - \beta_{V_1}S_1^EV_1^E - \mu S_1^E + a_2S_{20} = 0,\\
&\beta_{E_1}S_1^EE_1^E + \beta_{I_1}S_1^EI_1^E + \beta_{V_1}S_1^EV_1^E - (\alpha+\mu)E_1^E = 0,\\
&\alpha E_1^E - (w_1+\gamma+\mu)I_1^E = 0,\\
&\xi E_1^E - \sigma V_1^E = 0.
\end{aligned} \tag{4.7}$$

To establish the global asymptotic stability of x^E for the two-patch system, we only need to show that the positive equilibrium $(S_1^E, E_1^E, I_1^E, V_1^E)$ of system (4.6) is globally asymptotically stable in patch 1. We define a Lyapunov function

$$\begin{aligned}
\mathfrak{L} = &\int_{S_1^E}^{S_1} \frac{u-S_1^E}{u}du + \int_{E_1^E}^{E_1} \frac{u-E_1^E}{u}du + \frac{\beta_{I_1}S_1^EI_1^E}{\alpha E_1^E}\int_{I_1^E}^{I_1} \frac{u-I_1^E}{u}du\\
&+ \frac{\beta_{V_1}S_1^EV_1^E}{\xi E_1^E}\int_{V_1^E}^{V_1} \frac{u-V_1^E}{u}du.
\end{aligned}$$

We differentiate $\mathfrak{L}$ with respect to t along the solution of (4.6), and obtain

$$\mathfrak{L}' = (1-\frac{S_1^E}{S_1})S_1' + (1-\frac{E_1^E}{E_1})E_1' + \frac{\beta_{I_1}S_1^EI_1^E}{\alpha E_1^E}(1-\frac{I_1^E}{I_1})I_1' + \frac{\beta_{V_1}S_1^EV_1^E}{\xi E_1^E}(1-\frac{V_1^E}{V_1})V_1'.$$

Using the equations in (4.7), we then obtain

$$\begin{aligned}
\mathfrak{L}' = &(1-\frac{S_1^E}{S_1})[\Lambda_1 - \beta_{E_1}S_1E_1 - \beta_{I_1}S_1I_1 - \beta_{V_1}S_1V_1 - \mu S_1 + a_2S_{20}\\
&- (\Lambda_1 - \beta_{E_1}S_1^EE_1^E - \beta_{I_1}S_1^EI_1^E - \beta_{V_1}S_1^EV_1^E - \mu S_1^E + a_2S_{20})]\\
&\text{(denoted as } k_5)
\end{aligned}$$

$$+ (1 - \frac{E_1^E}{E_1})\{[\beta_{E_1}S_1E_1 + \beta_{I_1}S_1I_1 + \beta_{V_1}S_1V_1 - (\alpha+\mu)E_1] - [\beta_{E_1}S_1^EE_1^E + \beta_{I_1}S_1^EI_1^E + \beta_{V_1}S_1^EV_1^E - (\alpha+\mu)E_1^E]\} \quad \text{(denoted as } k_6)$$

$$+ \frac{\beta_{I_1}S_1^EI_1^E}{\alpha E_1^E}(1 - \frac{I_1^E}{I_1})\{[\alpha E_1 - (w_1+\gamma+\mu)I_1] - [\alpha E_1^E - (w_1+\gamma+\mu)I_1^E]\} \quad \text{(denoted as } k_7)$$

$$+ \frac{\beta_{V_1}S_1^EV_1^E}{\xi E_1^E}(1 - \frac{V_1^E}{V_1})[\xi E_1 - \sigma V_1 - (\xi E_1^E - \sigma V_1^E)]. \quad \text{(denoted as } k_8)$$

We arrange k_5, k_6, k_7 and k_8 separately as follows:

$$\begin{aligned}
k_5 =& \mu S_1^E(2 - \frac{S_1}{S_1^E} - \frac{S_1^E}{S_1}) + \beta_{E_1}(1 - \frac{S_1^E}{S_1})(S_1^EE_1^E - S_1E_1) \\
&+ \beta_{I_1}(1 - \frac{S_1^E}{S_1})(S_1^EI_1^E - S_1I_1) + \beta_{V_2}(1 - \frac{S_1^E}{S_1})(S_1^EV_1^E - S_1V_1) \\
=& \mu S_1^E(2 - \frac{S_1}{S_1^E} - \frac{S_1^E}{S_1}) \quad ✠_1 \\
&+ \beta_{E_1}[S_1^EE_1^E - S_1E_1 - \frac{(S_1^E)^2E_1^E}{S_1} + S_1^EE_1] \quad §_1 \\
&+ \beta_{I_1}[S_1^EI_1^E - S_1I_1 - \frac{(S_1^E)^2I_1^E}{S_1} + S_1^EI_1] \quad §_2 \\
&+ \beta_{V_1}[S_1^EV_1^E - S_1V_1 - \frac{(S_1^E)^2V_1^E}{S_1} + S_1^EV_1] \quad §_3, \\
k_6 =& (\alpha+\mu)E_1^E(2 - \frac{E_1}{E_1^E} - \frac{E_1^E}{E_1}) + \beta_{E_1}(1 - \frac{E_1^E}{E_1})(S_1E_1 - S_1^EE_1^E) \\
&+ \beta_{I_1}(1 - \frac{E_1^E}{E_1})(S_1I_1 - S_1^EI_1^E) + \beta_{V_1}(1 - \frac{E_1^E}{E_1})(S_1V_1 - S_1^EV_1^E) \\
=& (\alpha+\mu)E_1^E(2 - \frac{E_1}{E_1^E} - \frac{E_1^E}{E_1}) \quad ¶_1 \\
&+ \beta_{E_1}[-S_1^EE_1^E + S_1E_1 + \frac{S_1^E(E_1^E)^2}{E_1} - S_1E_1^E] \quad ‡_1 \\
&+ \beta_{I_1}[-S_1^EI_1^E + S_1I_1 - \frac{E_1^ES_1I_1}{E_1} + \frac{E_1^ES_1^EI_1^E}{E_1}] \quad ‡_2 \\
&+ \beta_{V_1}[-S_1^EV_1^E + S_1V_1 - \frac{E_1^ES_1V_1}{E_1} + \frac{E_1^ES_1^EV_1^E}{E_1}] \quad ‡_3, \\
k_7 =& \frac{\beta_{I_1}S_1^EI_1^E}{\alpha E_1^E}(\omega_1+\gamma+\mu)I_1^E(2 - \frac{I_1}{I_1^E} - \frac{I_1^E}{I_1}) \\
&+ \frac{\beta_{I_1}S_1^EI_1^E}{\alpha E_1^E}\alpha E_1^E(\frac{E_1}{E_1^E} - 1 - \frac{I_1^EE_1}{I_1E_1^E} + \frac{I_1^E}{I_1}) \\
=& \beta_{I_1}S_1^EI_1^E(1 - \frac{I_1}{I_1^E} + \frac{E_1}{E_1^E} - \frac{I_1^EE_1}{I_1E_1^E}) \quad ¥ \\
&\text{(on the basis of the third equation of (4.7)),}
\end{aligned}$$

and

$$\begin{aligned}k_8 &= \frac{\beta_{V_1} S_1^E V_1^E}{\xi E_1^E} \sigma V_1^E (2 - \frac{V_1^E}{V_1} - \frac{V_1}{V_1^E}) \\ &+ \frac{\beta_{V_1} S_1^E V_1^E}{\xi E_1^E} \xi E_1^E (\frac{E_1}{E_1^E} - 1 - \frac{V_1^E E_1}{V_1 E_1^E} + \frac{V_1^E}{V_1}) \\ &= \beta_{V_1} S_1^E V_1^E (1 - \frac{V_1}{V_1^E} + \frac{E_1}{E_1^E} - \frac{V_1^E E_1}{V_1 E_1^E}) \quad \pounds \\ &\quad \text{(according to the fourth equation of (4.7)).}\end{aligned}$$

We continue to organize the expressions for k_5, k_6, k_7 and k_8. First, we decompose the factor $¶_1$:

$$\begin{aligned}¶_1 &= (\beta_{E_1} S_1^E E_1^E + \beta_{I_1} S_1^E I_1^E + \beta_{V_1} S_1^E V_1^E)(2 - \frac{E_1}{E_1^E} - \frac{E_1^E}{E_1}) \\ &\quad \text{(due to the second equation of (4.7))} \\ &= \beta_{E_1} S_1^E E_1^E (2 - \frac{E_1}{E_1^E} - \frac{E_1^E}{E_1}) \quad ¶_{11} \\ &+ \beta_{I_1} S_1^E I_1^E (2 - \frac{E_1}{E_1^E} - \frac{E_1^E}{E_1}) \quad ¶_{12} \\ &+ \beta_{V_1} S_1^E V_1^E (2 - \frac{E_1}{E_1^E} - \frac{E_1^E}{E_1}) \quad ¶_{13}.\end{aligned}$$

Second, we combine the same items:

$$\begin{aligned}¶_{11} + §_1 + ‡_1 &= \beta_{E_1} S_1^E E_1^E (2 - \frac{E_1}{E_1^E} - \frac{E_1^E}{E_1} + \frac{E_1}{E_1^E} - \frac{S_1^E}{S_1} + \frac{E_1^E}{E_1} - \frac{S_1}{S_1^E}) \\ &= \beta_{E_1} S_1^E E_1^E (2 - \frac{S_1}{S_1^E} - \frac{S_1^E}{S_1}), \\ ¶_{12} + §_2 + ‡_2 + ¥ &= \beta_{I_1} S_1^E I_1^E (2 - \frac{E_1}{E_1^E} - \frac{E_1^E}{E_1} + 1 \\ &\quad + \frac{E_1}{E_1^E} + \frac{E_1^E}{E_1} - \frac{I_1^E E_1}{I_1 E_1^E} - \frac{S_1^E}{S_1} - \frac{E_1^E S_1 I_1}{E_1 S_1^E I_1^E}) \\ &= \beta_{I_1} S_1^E I_1^E (3 - \frac{I_1^E E_1}{I_1 E_1^E} - \frac{S_1^E}{S_1} - \frac{E_1^E S_1 I_1}{E_1 S_1^E I_1^E}),\end{aligned}$$

and

$$\begin{aligned}¶_{13} + §_3 + ‡_3 + \pounds &= \beta_{V_1} S_1^E V_1^E (2 - \frac{E_1}{E_1^E} - \frac{E_1^E}{E_1} + 1 \\ &\quad + \frac{E_1}{E_1^E} + \frac{E_1^E}{E_1} - \frac{V_1^E E_1}{V_1 E_1^E} - \frac{S_1^E}{S_1} - \frac{E_1^E S_1 V_1}{E_1 S_1^E V_1^E}) \\ &= \beta_{V_1} S_1^E V_1^E (3 - \frac{V_1^E E_1}{V_1 E_1^E} - \frac{S_1^E}{S_1} - \frac{E_1^E S_1 V_1}{E_1 S_1^E V_1^E}).\end{aligned}$$

Finally, adding the three equations above to the expression of $✠_1$, we obtain

$$\mathfrak{L}' = \mu S_1^E (2 - \frac{S_1}{S_1^E} - \frac{S_1^E}{S_1}) + \beta_{E_1} S_1^E E_1^E (2 - \frac{S_1}{S_1^E} - \frac{S_1^E}{S_1})$$

$$
\begin{aligned}
&+\beta_{I_1} S_1^E I_1^E (3 - \frac{I_1^E E_1}{I_1 E_1^E} - \frac{S_1^E}{S_1} - \frac{E_1^E S_1 I_1}{E_1 S_1^E I_1^E}) \\
&+\beta_{V_1} S_1^E V_1^E (3 - \frac{V_1^E E_1}{V_1 E_1^E} - \frac{S_1^E}{S_1} - \frac{E_1^E S_1 V_1}{E_1 S_1^E V_1^E}) \\
\le\, & 0.
\end{aligned}
$$

Meanwhile, it is easy to observe that the largest invariant set for $\mathfrak{L}' = 0$ is the singleton $\{(S_1^E, E_1^E, I_1^E, V_1^E)\}$. Hence, LaSalle's Invariance Principle yields that the positive equilibrium $(S_1^E, E_1^E, I_1^E, V_1^E)$ of the system (4.6) is globally asymptotically stable. We therefore conclude that the boundary equilibrium $x^E = (S_1^E, E_1^E, I_1^E, V_1^E, S_{20}, 0, 0, 0)$ of the two-patch system is globally asymptotically stable. □

Theorem 4.3. *When $\mathcal{R}_{01} < 1$ and $\mathcal{R}_{02} > 1$, the entire system has only two equilibria: the DFE x_0, and the endemic equilibrium x^{EE} defined in equation* (4.5). *When $\mathcal{R}_{01} > 1$ and $\mathcal{R}_{02} > 1$, the system has three equilibria: the DFE x_0, the boundary equilibrium x^E, and the endemic equilibrium x^{EE}. As long as $\mathcal{R}_{02} > 1$, the endemic equilibrium x^{EE} exists and is globally asymptotically stable.*

Proof. From the proof of Theorem 4.2, it is clear that the boundary equilibrium x^E does not exist when $\mathcal{R}_{01} < 1$. Now we show the existence and uniqueness of the endemic equilibrium x^{EE} when $\mathcal{R}_{02} > 1$. In this case, Theorem 3.1 states that the single-patch subsystem (2.2) has a unique endemic equilibrium $x_2^E = (S_2^E, E_2^E, I_2^E, V_2^E)$, defined in equation (3.8). Substitution of S_2^E and E_2^E into the first two equations of subsystem (2.1) at the equilibrium state yields a quadratic equation for E_1:

$$(\alpha + \mu) t_1 E_1^2 - [t_1 t_2 - \mu(\alpha + \mu)] E_1 - \mu b_2 E_2^E = 0, \tag{4.8}$$

where $t_1 = \beta_{E_1} + \beta_{I_1} \frac{\alpha}{\omega_1 + \gamma + \mu} + \beta_{V_1} \frac{\xi}{\sigma}$, and $t_2 = \Lambda_1 + a_2 S_2^E + b_2 E_2^E$. Obviously, equation (4.8) has one and only one positive real root, denoted by E_1^{EE}. Consequently, S_1^{EE}, I_1^{EE} and V_1^{EE} are uniquely determined from subsystem (2.1). Therefore, the two-patch system has a unique endemic equilibrium given by

$$x^{EE} = (S_1^{EE}, E_1^{EE}, I_1^{EE}, V_1^{EE}, S_2^E, E_2^E, I_2^E, V_2^E),$$

where $S_2^E = \frac{\alpha + \mu + b_2}{\beta_{E_2} + \beta_{V_2} \cdot \frac{\xi}{\sigma} + \frac{\alpha \beta_{I_2}}{w_2 + \gamma + \mu}}$, $E_2^E = \frac{\Lambda_2 - (\mu + a_2) S_2^E}{\alpha + \mu + b_2}$, $I_2^E = \frac{\alpha E_2^E}{w_2 + \gamma + \mu}$, $V_2^E = \frac{\xi E_2^E}{\sigma}$, $E_1^{EE} = \frac{t_1 t_2 - \mu(\alpha + \mu) + \sqrt{[t_1 t_2 - \mu(\alpha + \mu)]^2 + 4(\alpha + \mu) t_1 \mu b_2 E_2^E}}{2(\alpha + \mu) t_1}$, $S_1^{EE} = \frac{1}{\mu} \cdot [\Lambda_1 + a_2 S_2^E - (\alpha + \mu) E_1^{EE} + b_2 E_2^E]$, $I_1^{EE} = \frac{\alpha E_1^{EE}}{\omega_1 + \gamma + \mu}$, and $V_1^{EE} = \frac{\xi E_1^{EE}}{\sigma}$.

The proof of the global asymptotic stability of x^{EE} has some similarity to that of Theorem 4.2, and the details are provided in Appendix B. □

Theorems 4.1–4.3 provide a complete description of the global dynamics for our two-patch system (2.1) and (2.2). Biologically, these results highlight the role of the reproduction numbers associated with the two patches in characterizing the threshold between disease eradication and disease persistence. From a public health point of view, an outbreak control policy would need to reduce both $\mathcal{R}_{01}$ and $\mathcal{R}_{02}$ below unity; i.e., to meet the requirement of Theorem 4.1, in order to completely eliminate the infection.

5. Numerical results

We present some numerical simulation results in this section to illustrate the application of our modeling framework and to verify our analytical predictions. We fit our model to the publicly reported data in China from January 23rd to February 23rd that marked the most severe period of the COVID-19 epidemic in China, starting from the lockdown of Wuhan city (the epicenter) on January 23rd. We further divide this epidemic period into two stages: from January 23rd to February 3rd as the first stage, when the number of new infections reported daily was increasing; from February 4th to February 23rd as the second stage, when the number of daily new infections was decreasing. In particular, we mention the establishment of shelter hospitals in Hubei province around February 4th, which contributed significantly to the control of the epidemic and the decrease of new infections.

We conduct data fitting and numerical simulation for these two stages separately. For each stage, we fit our two-patch model to the daily reported new infections in Hubei province (patch 1) and the remaining part of China (patch 2). The results of our parameter estimation from data fitting are presented in Tables 1 and 2, respectively.

5.1. Stage 1 - from January 23rd to February 3rd

The curve fitting results for patch 1 and patch 2 are shown in Figure 1 and Figure 2, respectively. Based on the estimated parameter values from Tables 1, we can evaluate the reproduction numbers of the system. We find $\mathcal{R}_{01} = 5.382$ and $\mathcal{R}_{02} = 1.944$, where $\mathcal{R}_{01}$ and $\mathcal{R}_{02}$ are defined in equation (4.3). This result, where both reproduction numbers are higher than unity, is consistent with the onset and development of the disease outbreaks in both patches during this period of time. Meanwhile, we are also able to evaluate the environment-to-human transmission component in each of these two reproduction numbers, and we find $\mathcal{R}_{01}^{EH} = 0.409$, $\mathcal{R}_{02}^{EH} = 0.840$ (see equation (4.3)), which indicates a significant contribution from the environment-to-human transmission route toward the infection risk in each patch. The basic reproduction number for the entire system is given by $\mathcal{R}_0 = \max\{\mathcal{R}_{01}, \mathcal{R}_{02}\} = 5.382$ for this first stage of the epidemic.

In addition, we have sketched a phase portrait of I vs. E for each patch (see Figures 3 and 4) using the parameter values from Tables 1. We pick a set of different initial conditions, each of which determines a solution orbit. We observe that all these orbits converge to the endemic equilibrium over time, a demonstration of the globals asymptotic stability of the endemic equilibrium predicted in Theorem 4.3.

5.2. Stage 2 - from February 4th to February 23rd

Figure 5 and Figure 6 show the fitting results, respectively, for patch 1 and patch 2 in this period. Using the estimated parameter values from Tables 2, we find $\mathcal{R}_{01} = 0.558$, $\mathcal{R}_{02} = 0.209$, and thus $\mathcal{R}_0 = \max\{\mathcal{R}_{01}, \mathcal{R}_{02}\} = 0.558$. We also find $\mathcal{R}_{01}^{EH} = 0.0203$ and $\mathcal{R}_{02}^{EH} = 0.0855$. The result that $\mathcal{R}_0 < 1$ is a mathematical indication of the declining trend of the epidemic in China after February 4th, evidenced by the sustained reduction of the daily reported new infections.

Phase diagrams of I vs. E for the two patches with the parameter values in Tables 2 are presented in Figures 7 and 8. We observe that all the solution trajectories

Table 1. Definitions and values of model parameters from January 23rd to February 3rd

Parameter	Description	Value	Unit	Source
Λ_1	Population influx rate due to newborns in patch 1	1433.80325544	persons/day	[17]
β_{E_1}	Transmission constant between S and E in patch 1	6.45×10^{-9}	/person/day	Estimated
β_{I_1}	Transmission constant between S and I in patch 1	1.144×10^{-10}	/person/day	Estimated
β_{V_1}	Transmission constant between S and V in patch 1	1.008×10^{-10}	/virus/day	Estimated
μ	Natural death rate of human hosts in China	3.01×10^{-5}	per day	[13]
a_2	Rate of susceptible individuals moving from patch 2 to patch 1	2.9×10^{-6}	per day	Estimated
b_2	Rate of exposed individuals moving from patch 2 to patch 1	1.9×10^{-6}	per day	Estimated
ξ	Rate of the exposed contributing viruses to the environment	2.3	viruses/person/day	[13]
γ	Rate of recovery from infection	0.071428	per day	[13]
σ	Removal rate of the virus from the environment	0.42	per day	Estimated
ω_1	Disease-induced death rate in patch 1	0.01	per day	[13]
α^{-1}	Incubation period between infection and onset of symptoms	5.2	days	[7]
Λ_2	Population influx rate due to newborns in patch 2	32434.8697289	persons/day	[18]
β_{E_2}	Transmission constant between S and E in patch 2	9×10^{-13}	/person/day	Estimated
β_{I_2}	Transmission constant between S and I in patch 2	8×10^{-11}	/person/day	Estimated
β_{V_2}	Transmission constant between S and V in patch 2	3×10^{-11}	/virus/day	Estimated
ω_2	Disease-induced death rate in patch 2	1.7826×10^{-5}	per day	[13]
S_{10}	Initial value of the susceptible in patch 1	59270000	persons	[17]
E_{10}	Initial value of the exposed in patch 1	546	persons	[19]
I_{10}	Initial value of the infected in patch 1	525	persons	[19]
V_{10}	Initial value of viruses in the environment of patch 1	69279	viruses/ml	Estimated
S_{20}	Initial value of the susceptible in patch 2	1331600000	persons	[18]
E_{20}	Initial value of the exposed in patch 2	800	persons	[20]
I_{20}	Initial value of the infected in patch 2	246	persons	[20]
V_{20}	Initial value of viruses in the environment of patch 2	25150	viruses/ml	Estimated

converge to the disease-free equilibrium, an illustration of the global asymptotical stability of the DFE stated in Theorem 4.1.

Table 2. Definitions and values of model parameters from February 4th to February 23rd

Parameter	Description	Value	Unit	Source
β_{E_1}	Transmission constant between S and E in patch 1	5.6×10^{-10}	/person/day	Estimated
β_{I_1}	Transmission constant between S and I in patch 1	5.84×10^{-10}	/person/day	Estimated
β_{V_1}	Transmission constant between S and V in patch 1	2×10^{-11}	/virus/day	Estimated
a_2	Rate of susceptible individuals moving from patch 2 to patch 1	1.6×10^{-7}	per day	Estimated
b_2	Rate of exposed individuals moving from patch 2 to patch 1	2.3×10^{-7}	per day	Estimated
σ	Removal rate of the virus from the environment	0.63	per day	Estimated
β_{E_2}	Transmission constant between S and E in patch 2	8.7×10^{-14}	/person/day	Estimated
β_{I_2}	Transmission constant between S and I in patch 2	8.2×10^{-12}	/person/day	Estimated
β_{V_2}	Transmission constant between S and V in patch 2	4.2×10^{-12}	/virus/day	Estimated
E_{10}	Initial value of the exposed in patch 1	16411	persons	[19]
I_{10}	Initial value of the infected in patch 1	15679	persons	[19]
E_{20}	Initial value of the exposed in patch 2	3801	persons	[20]
I_{20}	Initial value of the infected in patch 2	7263	persons	[20]

In addition, Figures 9 and 10 show a long-term simulation for the epidemic development of COVID-19 in the two patches of China, based on our model. We observe that the prevalence levels (I_1 and I_2) both increase initially, reaching a peak around February 6th in patch 2 and around February 9th in patch 1, and then start decreasing. It takes about 6 months for patch 2 to reach a state of almost complete elimination of the disease (with the number of infections below 1), whereas it takes about 12 months for patch 1 to reach the same level of disease elimination. An indication is that patch 1 (Hubei province) has a higher degree of outbreak severity and a longer period of disease persistence than patch 2 (other parts of China) does, so that stronger disease control measures may be always needed in Hubei province

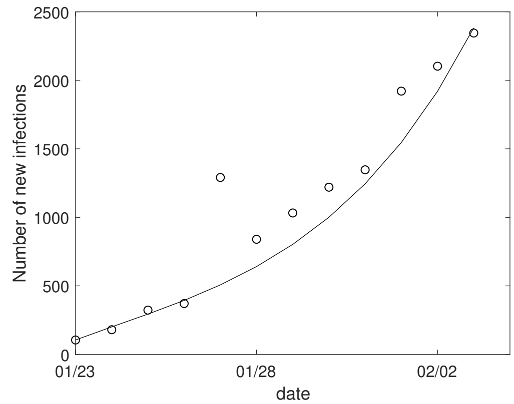

Figure 1. Data fitting for the daily new infections from January 23rd to February 3rd in patch 1. The circles represent the reported data and the solid line represents the fitting result.

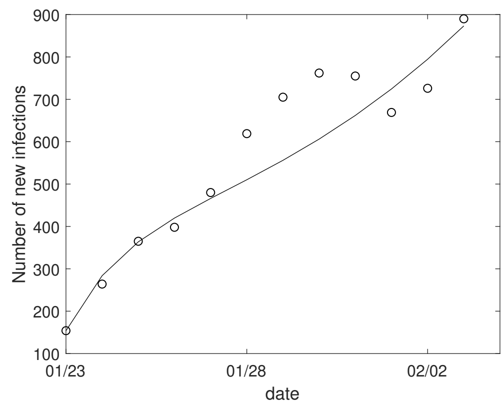

Figure 2. Data fitting for the daily new infections from January 23rd to February 3rd in patch 2. The circles represent the reported data and the solid line represents the fitting result.

compared to those in other parts of the country.

5.3. Infection risks versus communication rates

Finally, we make some discussion regarding the impact of the parameters a_2 and b_2 on the disease risks. Our model has two patches and a_2 and b_2, which quantify the rates of population movement, represent the communication between the two patches (in a unidirectional manner) and contribute to the heterogeneity in different parts of the country.

The infection risks for the two patches are measured by their reproduction numbers $\mathcal{R}_{01}$ and $\mathcal{R}_{02}$. To quantify their dependence on the communication rates, we calculate their partial derivatives with respect to a_2 and b_2 and list the results in Table 3. Note that since $\mathcal{R}_{01}$ does not depend on b_2, $\frac{\partial \mathcal{R}_{01}}{\partial b_2} = 0$ which is not displayed in the table. We observe that $\mathcal{R}_{01}$ increases monotonically with respect to a_2, whereas $\mathcal{R}_{02}$ decreases monotonically with both a_2 and b_2, an indication that the unidirectional population movement tends to reduce the disease risk for patch

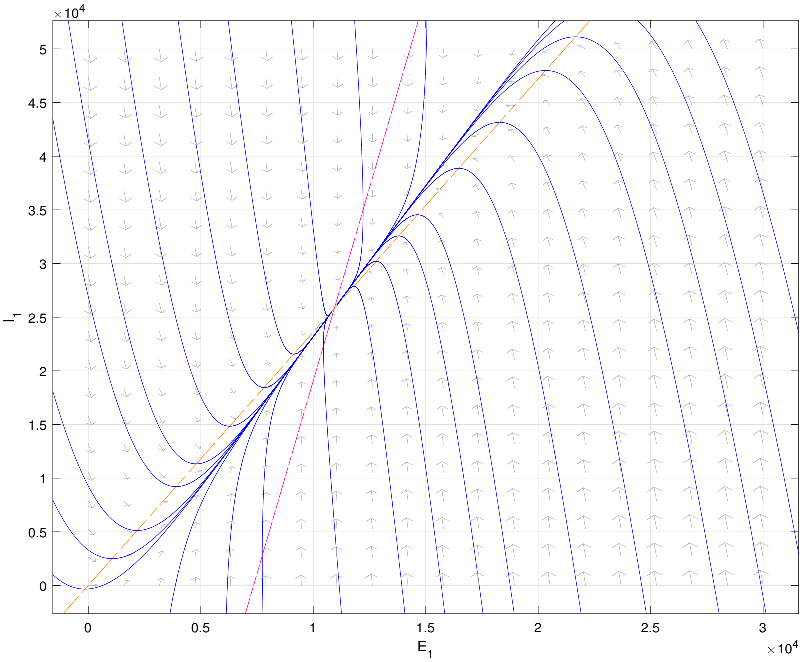

Figure 3. The phase diagram of I_1 vs. E_1 in patch 1 based on the parameter setting in stage 1 (from January 23rd to February 3rd). The trajectories starting from different initial values approach the endemic equilibrium where (E_1^{EE}, I_1^{EE})=(10940, 25826).

2 but increase the risk for patch 1. Moreover, Figure 11 illustrates how the two reproduction numbers change when a_2 and b_2 vary in some ranges. As shown in the figure, $\mathcal{R}_{01}$ is more sensitive than $\mathcal{R}_{02}$ to the change of a_2, and $\mathcal{R}_{02}$ is more sensitive with respect to the change of a_2 than that of b_2.

These results imply that for the outbreak management, there could be a conflict between different parts of the country in terms of mobility control, as host movement may reduce the infection risk for one patch but increase the risk for the other. Incorporation of such a mobility factor as well as other spatial heterogeneity characteristics could help with the public health policy development that better balances the disease control efforts in different regions, and with the strategy design that makes the overall epidemic prevention and intervention more effective.

Table 3. Dependence of reproduction numbers on communication raes

Symbol	Expression	Property
$\mathcal{R}_{01}$	$\frac{\beta_{E_1}+\frac{\alpha\beta_{I_1}}{\omega_1+\gamma+\mu}+\frac{\xi\beta_{V_1}}{\sigma}}{\mu(\alpha+\mu)}\cdot(\Lambda_1+\frac{\Lambda_2 a_2}{\mu+a_2})$	Increasing
$\frac{\partial\mathcal{R}_{01}}{\partial a_2}$	$\frac{\Lambda_2\cdot(\beta_{E_1}+\frac{\alpha\beta_{I_1}}{\omega_1+\gamma+\mu}+\frac{\xi\beta_{V_1}}{\sigma})}{\alpha+\mu}\cdot\frac{1}{(\mu+a_2)^2}$	>0
$\mathcal{R}_{02}$	$\frac{\beta_{E_2}+\frac{\alpha\beta_{I_2}}{\omega_2+\gamma+\mu}+\frac{\xi\beta_{V_2}}{\sigma}}{\alpha+\mu+b_2}\cdot(\frac{\Lambda_2}{\mu+a_2})$	Decreasing
$\frac{\partial\mathcal{R}_{02}}{\partial a_2}$	$\frac{\Lambda_2\cdot(\beta_{E_2}+\frac{\alpha\beta_{I_2}}{\omega_2+\gamma+\mu}+\frac{\xi\beta_{V_2}}{\sigma})}{\alpha+\mu+b_2}\cdot[-\frac{1}{(\mu+a_2)^2}]$	<0
$\frac{\partial\mathcal{R}_{02}}{\partial b_2}$	$\frac{\Lambda_2\cdot(\beta_{E_2}+\frac{\alpha\beta_{I_2}}{\omega_2+\gamma+\mu}+\frac{\xi\beta_{V_2}}{\sigma})}{\mu+a_2}\cdot[-\frac{1}{(\alpha+\mu+b_2)^2}]$	<0

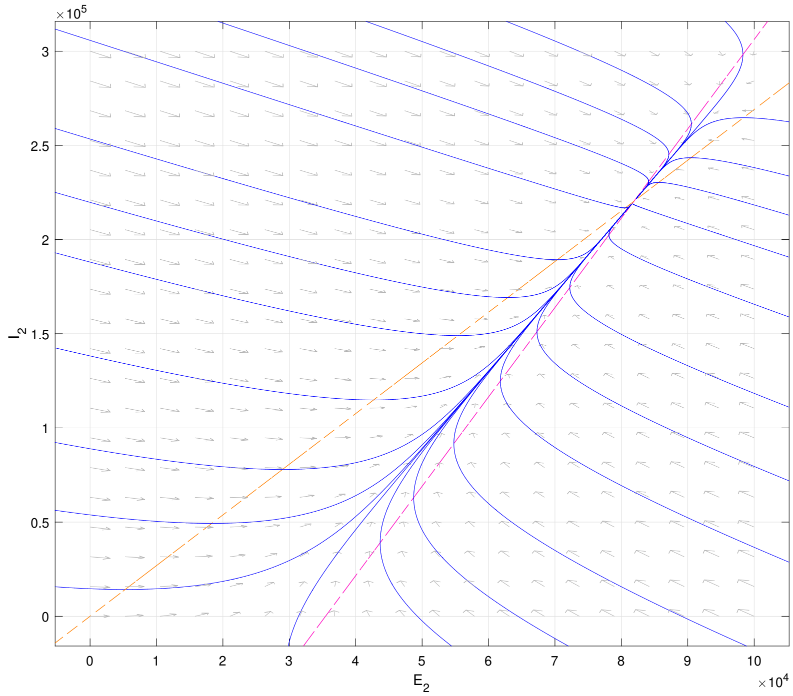

Figure 4. The phase diagram of I_2 vs. E_2 in patch 2 based on the parameter setting in stage 1 (from January 23rd to February 3rd). The trajectories starting from different initial values approach the endemic equilibrium where $(E_2^E,\ I_2^E)$=(81893, 220326).

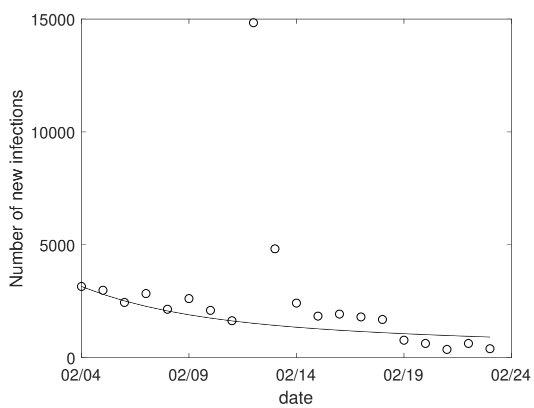

Figure 5. Data fitting for the daily new infections from February 4th to February 23rd in patch 1. The circles represent the reported data and the solid line represents the fitting result.

6. Conclusion

We have presented a two-patch model for the transmission dynamics of COVID-19 in China. This two-patch structure is based on the observation that Hubei province, associated with more than 80% of the cases reported in China, has significantly higher disease prevalence and infection risk than any other part of the country.

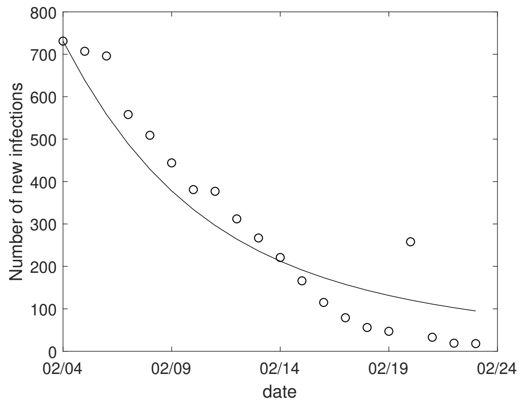

Figure 6. Data fitting for the daily new infections from February 4th to February 23rd in patch 2. The circles represent the reported data and the solid line represents the fitting result.

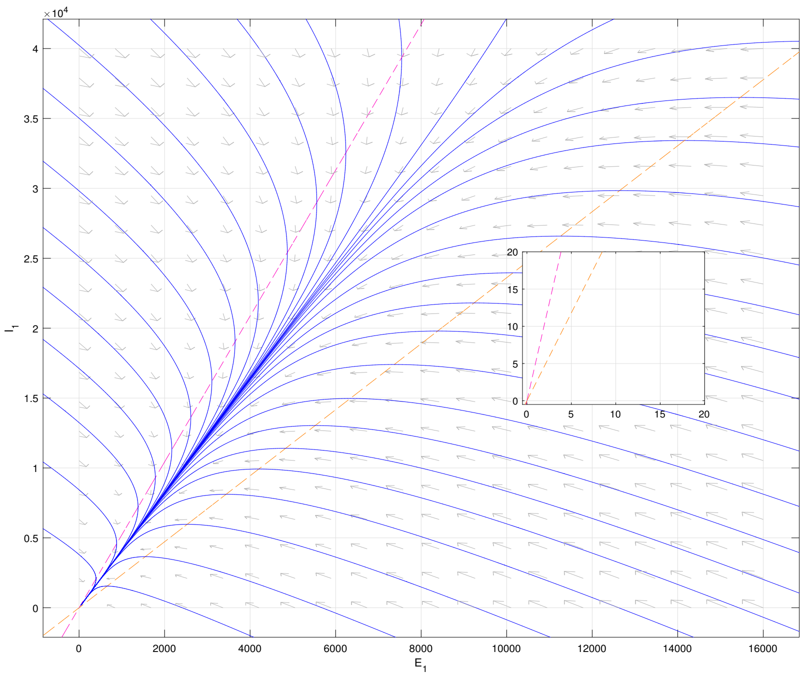

Figure 7. The phase diagram of I_1 vs. E_1 in patch 1 based on the parameter setting in stage 2 (from February 4th to February 23rd). The trajectories starting from different initial values approach the disease-free equilibrium where $(E_{10}^*,\ I_{10}^*)$=(0, 0).

Our model incorporates different parameter settings for the two patches and takes into account the population movement, emphasizing the spatial heterogeneity in disease dynamics. Meanwhile, our model includes both the human-to-human and environment-to-human transmission routes, highlighting the importance of the environment in the transmission and spread of this disease.

Through a careful equilibrium analysis, we have established the global stabilities for both the single-patch subsystem and the entire two-patch system. Our results

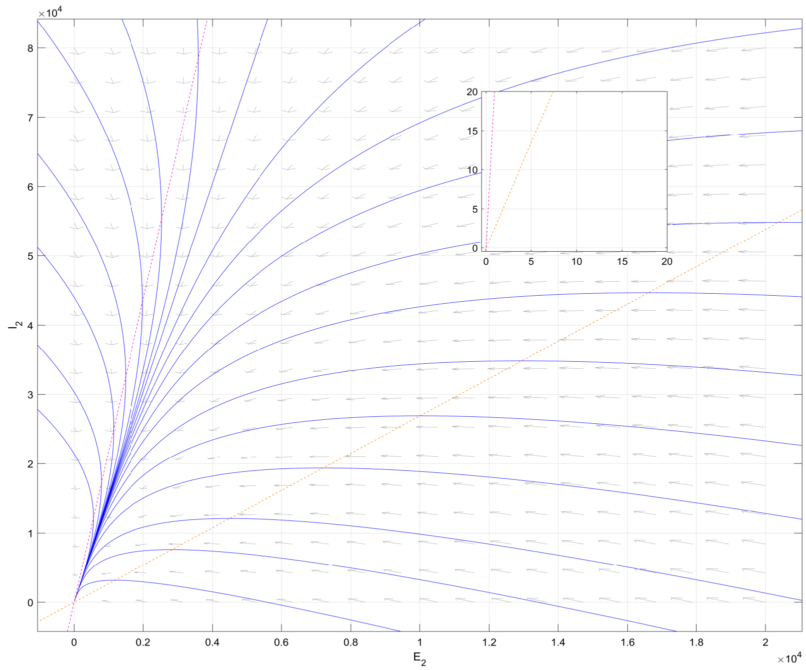

Figure 8. The phase diagram of I_2 vs. E_2 in patch 2 based on the parameter setting in stage 2 (from February 4th to February 23rd). The trajectories starting from different initial values approach the disease-free equilibrium where $(E_{20}^*, I_{20}^*)=(0, 0)$.

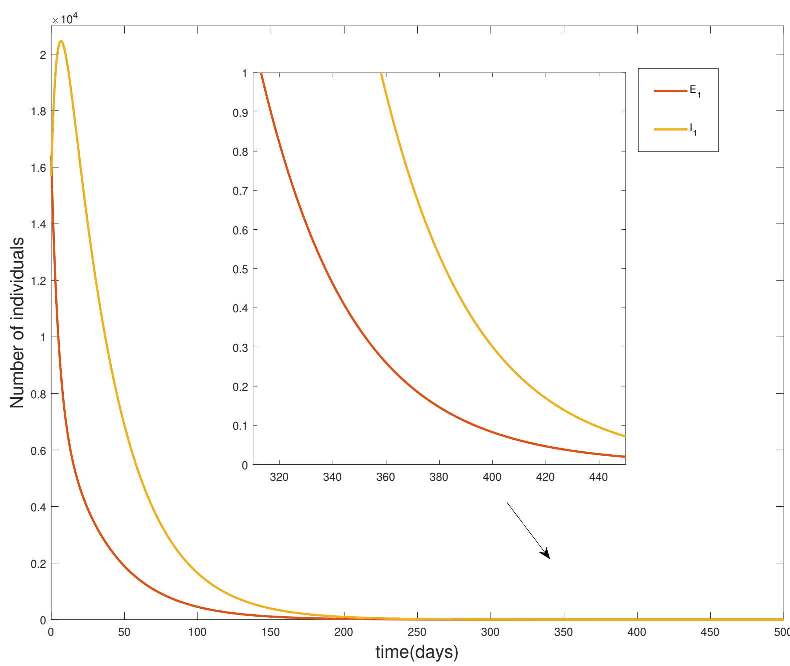

Figure 9. Long-term simulation for the numbers of exposed and infected individuals in patch 1.

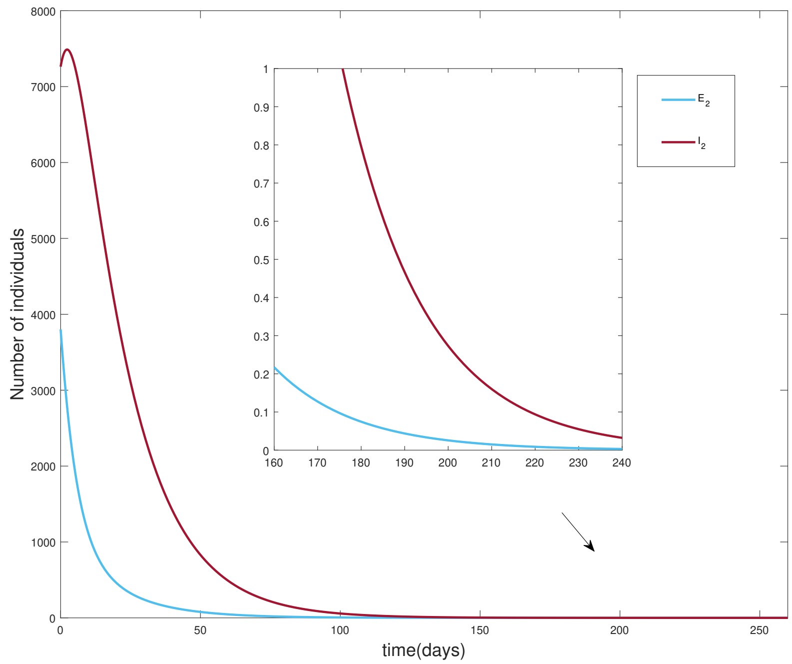

Figure 10. Long-term simulation for the numbers of exposed and infected individuals in patch 2.

show that the reproduction numbers in each case can be used to characterize the disease threshold: when the reproduction number is lower than unity, the disease-free equilibrium is globally asymptotically stable in the relevant region; when it is higher than unity, the endemic equilibrium is globally asymptotically stable in the relevant region. Rich dynamics occur with the interaction between the two patches and we find that the disease could be completely eradicated (if $\mathcal{R}_{01} < 1$ and $\mathcal{R}_{02} < 1$), could die out in patch 2 but become endemic in patch 1 (if $\mathcal{R}_{02} < 1$ and $\mathcal{R}_{01} > 1$), and could persist in both patches (if $\mathcal{R}_{02} > 1$).

When our model is applied to the reported data in China, we find that the reproduction numbers for both patches are higher than unity during January 23 to February 4, but both are reduced below unity afterwards, indicating an elimination of the infection in the long run. Our numerical simulation results are in line with this finding. Meanwhile, we observe that $\mathcal{R}_{01}$, the reproduction number for patch 1, is much higher than $\mathcal{R}_{02}$, the reproduction number for patch 2, consistent with the fact that patch 1 (i.e., Hubei province) represents the vast majority of the reported cases in China and has a higher risk than that of the remaining part of the country. Through data fitting, we find that for each patch, the contribution from the environment-to-human transmission route is significant toward the overall infection risk. This provides a justification of the indirect transmission pathway incorporated in our model. We also find that the communication rates, represented by the parameters a_2 and b_2, between the two patches play an important role in shaping the overall disease risk. Specifically, population movement from patch 2 to patch 1 reduces the risk for patch 2, but increases the risk for patch 1. Disease control policies shall take into account this observation, so as to optimally scale the intervention efforts in different regions and manage the outbreak in a holistic

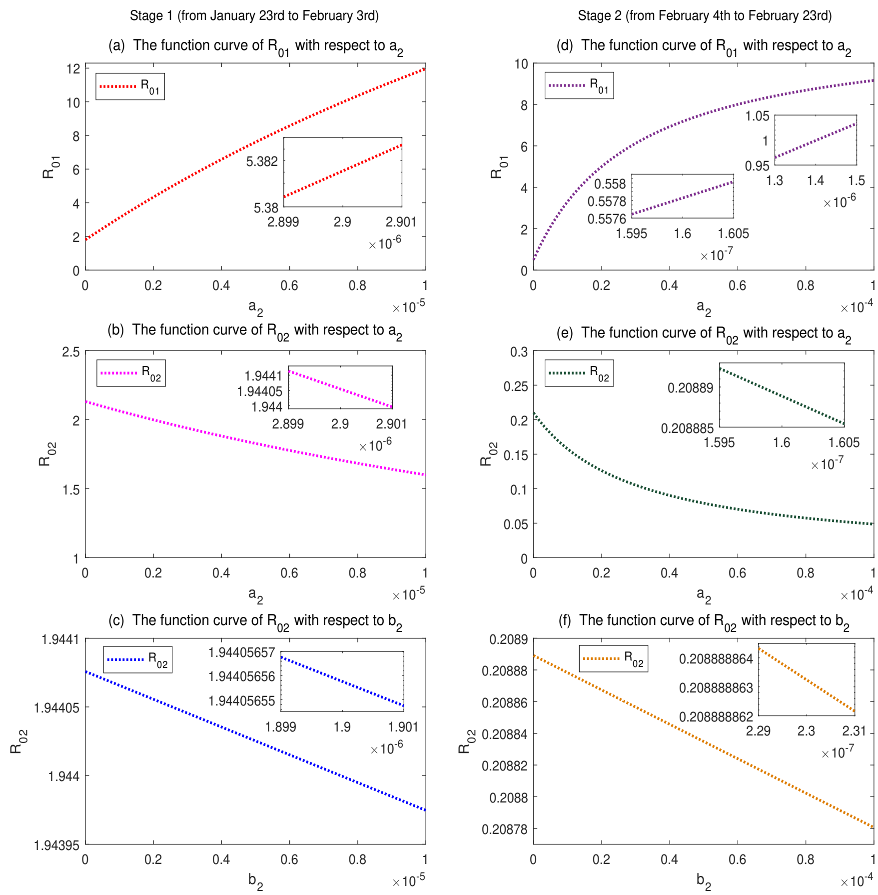

Figure 11. The impact of the population movement rates a_2 and b_2 on the reproduction numbers $\mathcal{R}_{01}$ and $\mathcal{R}_{02}$. Left panel: stage 1 (January 23rd – February 3rd); right panel: stage 2 (February 4th – February 23rd).

manner.

This paper represents a pilot study for the spatial heterogeneity of COVID-19 transmission, in a coarse-grained, two-patch setting. A natural extension is to formulate a multi-patch model that could accommodate a large number of patches. Application of this extended model to a country, such as China or the US, with each patch representing one province or state, will possibly lead to a better description of the COVID-19 transmission dynamics in a heterogeneous environment.

Acknowledgements

We would like to thank the reviewers for providing valuable comments and the editors for handling this manuscript.

Appendix A: Local stability of the endemic equilibrium in patch 2

We study the local asymptotic stability of the endemic equilibrium $x_2^E=(S_2^E,\ E_2^E,\ I_2^E,\ V_2^E)$ for the subsystem (2.2) when $\mathcal{R}_{02} > 1$. Evaluating the Jacobian matrix at x_2^E, we obtain

$$\begin{pmatrix} a_{11} & -\beta_{E_2}S_2^E & -\beta_{I_2}S_2^E & -\beta_{V_2}S_2^E \\ a_{21} & a_{22} & \beta_{I_2}S_2^E & \beta_{V_2}S_2^E \\ 0 & \alpha & -(\omega_2+\gamma+\mu) & 0 \\ 0 & \xi & 0 & -\sigma \end{pmatrix},$$

where $a_{11} = -\beta_{E_2}E_2^E - \beta_{I_2}I_2^E - \beta_{V_2}V_2^E - \mu - a_2$, $a_{21} = \beta_{E_2}E_2^E + \beta_{I_2}I_2^E + \beta_{V_2}V_2^E$, $a_{22} = \beta_{E_2}S_2^E - (\alpha+\mu+b_2)$. Its characteristic polynomial is given by

$$\det(\lambda I - \tilde{J}) = \lambda^4 + c_1\lambda^3 + c_2\lambda^2 + c_3\lambda + c_4,$$

where

$$\begin{aligned} c_1 &= l_1 + d_3 + d_2, \\ c_2 &= l_2 + d_3 l_1 + d_2(q_2+\sigma+d_1), \\ c_3 &= l_3 + d_3 l_2 + d_2(q_2\sigma + d_1 q_2 + d_1\sigma), \\ c_4 &= d_3 l_3 + d_2 d_1 q_2 \sigma, \end{aligned}$$

with

$$\begin{aligned} l_1 &= q_1 + q_2 + \sigma, \\ l_2 &= q_1 q_2 + \sigma(q_1+q_2) - (q_3+q_4), \\ l_3 &= \sigma q_1 q_2 - \sigma q_3 - q_4 q_2, \end{aligned}$$

and

$$\begin{aligned} q_1 &= -\beta_{E_2}S_2^E + \alpha + \mu + b_2, \\ q_2 &= \omega_2 + \gamma + \mu, \\ q_3 &= \alpha\beta_{I_2}S_2^E, \\ q_4 &= \xi\beta_{V_2}S_2^E, \\ d_1 &= \alpha + \mu + b_2, \\ d_2 &= \beta_{E_2}E_2^E + \beta_{I_2}I_2^E + \beta_{V_2}V_2^E, \\ d_3 &= \mu + a_2. \end{aligned}$$

Thus, the stability of the endemic equilibrium x^E is determined by the zeros of

$$\lambda^4 + c_1\lambda^3 + c_2\lambda^2 + c_3\lambda + c_4 = 0.$$

It follows from the Routh-Hurwitz criterion that to verify the stability of x_2^E, it suffices to show

$$c_1 > 0,\quad c_2 > 0,\quad c_3 > 0,\quad c_4 > 0,\quad c_1c_2 - c_3 > 0,\quad c_1c_2c_3 - c_1^2c_4 - c_3^2 > 0.$$

Firstly, note that

$$\begin{aligned} q_1 = & -\beta_{E_2} S_2^E + \alpha + \mu + b_2 \\ = & -\beta_{E_2} \frac{\alpha + \mu + b_2}{\beta_{E_2} + \beta_{V_2} \cdot \frac{\xi}{\sigma} + \frac{\alpha \beta_{I_2}}{w_2 + \gamma + \mu}} + \alpha + \mu + b_2 \\ = & (\alpha + \mu + b_2)(1 - \frac{\beta_{E_2}}{\beta_{E_2} + \beta_{V_2} \cdot \frac{\xi}{\sigma} + \frac{\alpha \beta_{I_2}}{w_2 + \gamma + \mu}}) \\ > & 0, \end{aligned}$$

which leads to

$$l_1 = q_1 + q_2 + \sigma > 0,$$

and

$$c_1 = l_1 + d_3 + d_2 > 0.$$

Secondly, note that

$$\begin{aligned} l_2 = & q_1 q_2 + \sigma(q_1 + q_2) - (q_3 + q_4) \\ = & -S_2^E[(q_2 + \sigma)\beta_{E_2} + \alpha\beta_{I_2} + \xi\beta_{V_2}] + (\alpha + \mu + b_2)(q_2 + \sigma) + \sigma q_2 \\ = & \frac{\alpha + \mu + b_2}{\beta_{E_2} + \beta_{V_2} \cdot \frac{\xi}{\sigma} + \beta_{I_2} \cdot \frac{\alpha}{w_2 + \gamma + \mu}} \cdot \\ & [(q_2 + \sigma)\beta_{E_2} + q_2 \beta_{V_2} \frac{\xi}{\sigma} + \xi\beta_{V_2} + \alpha\beta_{I_2} + \sigma\beta_{I_2} \frac{\alpha}{w_2 + \gamma + \mu} \\ & -(q_2 + \sigma)\beta_{E_2} - \alpha\beta_{I_2} - \xi\beta_{V_2}] + \sigma q_2 \\ = & S_2^E(q_2 \beta_{V_2} \frac{\xi}{\sigma} + \sigma\beta_{I_2} \frac{\alpha}{w_2 + \gamma + \mu}) + \sigma q_2 \\ > & 0, \end{aligned}$$

which leads to

$$c_2 = l_2 + d_3 l_1 + d_2(q_2 + \sigma + d_1) > 0.$$

Thirdly, note that

$$\begin{aligned} l_3 = & \sigma(q_1 q_2 - q_3) - q_4 q_2 \\ = & \frac{\alpha + \mu + b_2}{\beta_{E_2} + \beta_{V_2} \cdot \frac{\xi}{\sigma} + \beta_{I_2} \cdot \frac{\alpha}{w_2 + \gamma + \mu}} \cdot \\ & [-\sigma\beta_{E_2}(w_2 + \gamma + \mu) - \sigma\alpha\beta_{I_2} - \xi(w_2 + \gamma + \mu)\beta_{V_2} + \\ & \sigma\beta_{E_2}(w_2 + \gamma + \mu) + \sigma\alpha\beta_{I_2} + \xi(w_2 + \gamma + \mu)\beta_{V_2}] \\ = & 0, \end{aligned}$$

which leads to

$$c_3 = l_3 + d_3 l_2 + d_2(q_2 \sigma + d_1 q_2 + d_1 \sigma) > 0,$$

and

$$c_4 = \ d_3 l_3 + d_2 d_1 q_2 \sigma > 0.$$

Next, we have

$$\begin{aligned}
c_1 c_2 - c_3 =& (l_1 + d_3 + d_2)[l_2 + d_3 l_1 + d_2(q_2 + \sigma + d_1)] \\
& - [l_3 + d_3 l_2 + d_2(q_2 \sigma + d_1 q_2 + d_1 \sigma)] \\
=& l_1 l_2 + d_2 l_2 + l_1^2 d_3 + d_3^2 l_1 + d_2 d_3 l_1 + (q_1 + q_2) d_2 q_2 + l_1 d_2 \sigma + q_1 d_2 d_1 \\
& + (d_2 + d_3) d_2 (q_2 + \sigma + d_1) \\
>& 0.
\end{aligned}$$

Moreover, after direct calculation, we obtain

$$\begin{aligned}
& c_1 c_2 c_3 - c_1^2 c_4 - c_3^2 \\
=& c_3(c_1 c_2 - c_3) - c_1^2 c_4 \\
=& [d_3 l_2 + d_2(q_2 \sigma + d_1 q_2 + d_1 \sigma)] \cdot [l_1 l_2 + d_2 l_2 + l_1^2 d_3 + d_3^2 l_1 + d_2 d_3 l_1 \\
& + (q_1 + q_2) d_2 q_2 + l_1 d_2 \sigma + q_1 d_2 d_1 + (d_2 + d_3) d_2 (q_2 + \sigma + d_1)] \\
& - (l_1 + d_3 + d_2)^2 d_2 d_1 q_2 \sigma \\
=& d_3 l_2 \cdot [l_1 l_2 + d_2 l_2 + l_1^2 d_3 + d_3^2 l_1 + d_2 d_3 l_1 \\
& + (q_1 + q_2) d_2 q_2 + l_1 d_2 \sigma + q_1 d_2 d_1 + (d_2 + d_3) d_2 (q_2 + \sigma + d_1)] \\
& + d_2(q_2 \sigma + d_1 q_2 + d_1 \sigma) \cdot [l_1 l_2 + d_2 l_2 + l_1^2 d_3 + d_3^2 l_1 + d_2 d_3 l_1 \\
& + (q_1 + q_2) d_2 q_2 + l_1 d_2 \sigma + q_1 d_2 d_1 + (d_2 + d_3) d_2 (q_2 + \sigma + d_1)] \\
& - (l_1^2 + d_3^2 + d_2^2 + 2 l_1 d_3 + 2 l_1 d_2 + 2 d_2 d_3) d_2 d_1 q_2 \sigma \\
=& d_3 l_2 \cdot [l_1 l_2 + d_2 l_2 + l_1^2 d_3 + d_3^2 l_1 + d_2 d_3 l_1 \\
& + (q_1 + q_2) d_2 q_2 + l_1 d_2 \sigma + q_1 d_2 d_1 + (d_2 + d_3) d_2 (q_2 + \sigma + d_1)] \\
& + d_2(q_2 \sigma + d_1 q_2 + d_1 \sigma) \cdot \{l_1 l_2 + d_2[S_2^E(q_2 \beta_{V_2} \frac{\xi}{\sigma} + \sigma \beta_{I_2} \frac{\alpha}{w_2 + \gamma + \mu}) + \sigma q_2] \\
& + l_1 d_3 (q_1 + q_2 + \sigma) + d_3^2 (q_1 + q_2 + \sigma) + d_2 d_3 l_1 \\
& + (q_1 + q_2) d_2 q_2 + l_1 d_2 \sigma + q_1 d_2 d_1 + (d_2 + d_3) d_2 (q_2 + \sigma + d_1)\} \\
& - (l_1^2 + d_3^2 + d_2^2 + 2 l_1 d_3 + 2 l_1 d_2 + 2 d_2 d_3) \cdot d_2 d_1 q_2 \sigma \\
=& m_1 + m_2 + m_3 + m_4 + m_5 + d_2 d_3 l_1 + q_1 d_2 d_1 + m_6,
\end{aligned}$$

with

$$\begin{aligned}
m_1 =& d_3 l_2 \cdot [l_1 l_2 + d_2 l_2 + l_1^2 d_3 + d_3^2 l_1 + d_2 d_3 l_1 \\
& + (q_1 + q_2) d_2 q_2 + l_1 d_2 \sigma + q_1 d_2 d_1 + (d_2 + d_3) d_2 (q_2 + \sigma + d_1)], \\
m_2 =& d_2(q_2 \sigma + d_1 q_2 + d_1 \sigma) \cdot l_1 l_2 - l_1^2 \cdot d_2 d_1 q_2 \sigma \\
=& d_2(q_2 \sigma + d_1 q_2 + d_1 \sigma) \cdot l_1 [S_2^E(q_2 \beta_{V_2} \frac{\xi}{\sigma} + \sigma \beta_{I_2} \frac{\alpha}{w_2 + \gamma + \mu}) + \sigma q_2] \\
& - l_1 (q_1 + q_2 + \sigma) \cdot d_2 d_1 q_2 \sigma \\
=& d_2(q_2 \sigma + d_1 q_2 + d_1 \sigma) \cdot l_1 S_2^E(q_2 \beta_{V_2} \frac{\xi}{\sigma} + \sigma \beta_{I_2} \frac{\alpha}{w_2 + \gamma + \mu}) \\
& + d_2(q_2 \sigma + d_1 q_2) \cdot l_1 \sigma q_2 - l_1 (q_1 + q_2) \cdot d_2 d_1 q_2 \sigma
\end{aligned}$$

$$
\begin{aligned}
&=d_2(q_2\sigma+d_1q_2+d_1\sigma)\cdot l_1S_2^E(q_2\beta_{V_2}\frac{\xi}{\sigma}+\sigma\beta_{I_2}\frac{\alpha}{w_2+\gamma+\mu})\\
&\quad+d_2q_2\sigma\cdot l_1\sigma q_2-l_1q_1\cdot d_2d_1q_2\sigma\\
&=d_2(q_2\sigma+d_1q_2+d_1\sigma)\cdot l_1S_2^E(q_2\beta_{V_2}\frac{\xi}{\sigma}+\sigma\beta_{I_2}\frac{\alpha}{w_2+\gamma+\mu})\\
&\quad+d_2q_2\sigma\cdot l_1\sigma q_2-l_1(-\beta_{E_2}S_2^E+d_1)\cdot d_2d_1q_2\sigma\\
&=d_2(q_2\sigma+d_1q_2+d_1\sigma)\cdot l_1S_2^E(q_2\beta_{V_2}\frac{\xi}{\sigma}+\sigma\beta_{I_2}\frac{\alpha}{w_2+\gamma+\mu})\\
&\quad+l_1\beta_{E_2}S_2^E\cdot d_2d_1q_2\sigma+d_2q_2\sigma\cdot l_1\sigma q_2-l_1d_1\cdot d_2d_1q_2\sigma\\
&\quad\text{(the positivity of } m_2 \text{ will be discussed later)},\\
m_3&=d_2(q_2\sigma+d_1q_2+d_1\sigma)\cdot\{d_2[S_2^E(q_2\beta_{V_2}\frac{\xi}{\sigma}+\sigma\beta_{I_2}\frac{\alpha}{w_2+\gamma+\mu})+\sigma q_2]\\
&\quad+(q_1+q_2)d_2q_2+l_1d_2\sigma\}-2l_1d_2\cdot d_2d_1q_2\sigma\\
&=d_2(q_2\sigma+d_1q_2+d_1\sigma)\cdot\{d_2S_2^E(q_2\beta_{V_2}\frac{\xi}{\sigma}+\sigma\beta_{I_2}\frac{\alpha}{w_2+\gamma+\mu})\\
&\quad+l_1d_2q_2+l_1d_2\sigma\}-2l_1d_2\cdot d_2d_1q_2\sigma\\
&=d_2(q_2\sigma+d_1q_2+d_1\sigma)\cdot d_2S_2^E(q_2\beta_{V_2}\frac{\xi}{\sigma}+\sigma\beta_{I_2}\frac{\alpha}{w_2+\gamma+\mu})\\
&\quad+d_2(q_2\sigma+d_1q_2)\cdot l_1d_2q_2+d_2(q_2\sigma+d_1\sigma)\cdot l_1d_2\sigma,\\
m_4&=d_2(q_2\sigma+d_1q_2+d_1\sigma)\cdot l_1d_3(q_1+q_2+\sigma)-2l_1d_3\cdot d_2d_1q_2\sigma\\
&=d_2(q_2\sigma+d_1q_2+d_1\sigma)\cdot l_1d_3(q_1+\sigma)+d_2(q_2\sigma+d_1q_2)\cdot l_1d_3q_2\\
&\quad+d_2(q_2\sigma+d_1q_2+d_1\sigma)\cdot l_1d_3(q_1+q_2)+d_2(q_2\sigma+d_1\sigma)\cdot l_1d_3\sigma,\\
m_5&=d_2(q_2\sigma+d_1q_2+d_1\sigma)\cdot d_3^2(q_1+q_2+\sigma)-d_3^2\cdot d_2d_1q_2\sigma\\
&=d_2(q_2\sigma+d_1q_2+d_1\sigma)\cdot d_3^2(q_1+\sigma)+d_2(q_2\sigma+d_1q_2)\cdot d_3^2q_2,\\
m_6&=d_2(q_2\sigma+d_1q_2+d_1\sigma)\cdot(d_2+d_3)d_2(q_2+\sigma+d_1)-(d_2^2+2d_2d_3)\cdot d_2d_1q_2\sigma\\
&=d_2(q_2\sigma+d_1q_2+d_1\sigma)\cdot(d_2^2q_2+d_2^2\sigma+d_2^2d_1+d_3d_2q_2+d_3d_2\sigma+d_3d_2d_1)\\
&\quad-(d_2^2\cdot d_2d_1q_2\sigma+2d_2d_3\cdot d_2d_1q_2\sigma)\\
&=d_2(q_2\sigma+d_1q_2+d_1\sigma)\cdot(d_2^2\sigma+d_2^2d_1)+d_2(q_2\sigma+d_1q_2)\cdot d_2^2q_2\\
&\quad+d_2(q_2\sigma+d_1q_2+d_1\sigma)\cdot(d_3d_2\sigma+d_3d_2d_1)+d_2(q_2\sigma+d_1q_2)\cdot d_3d_2q_2\\
&\quad+d_2(q_2\sigma+d_1q_2+d_1\sigma)\cdot(d_3d_2q_2+d_3d_2\sigma)+d_2(d_1q_2+d_1\sigma)\cdot d_3d_2d_1.
\end{aligned}
$$

For the positivity of m_2, we give an explanation as follows:

(i)if $\sigma\geq q_2$,

$$
\begin{aligned}
m_2&=d_2(q_2\sigma+d_1q_2+d_1\sigma)\cdot l_1S_2^E(q_2\beta_{V_2}\frac{\xi}{\sigma}+\sigma\beta_{I_2}\frac{\alpha}{w_2+\gamma+\mu})\\
&\quad+l_1\beta_{E_2}S_2^E\cdot d_2d_1q_2\sigma+d_2q_2\sigma\cdot l_1\sigma q_2-l_1d_1\cdot d_2d_1q_2\sigma\\
&=d_2(q_2\sigma+d_1q_2)\cdot l_1S_2^E(q_2\beta_{V_2}\frac{\xi}{\sigma}+\sigma\beta_{I_2}\frac{\alpha}{w_2+\gamma+\mu})+d_2q_2\sigma\cdot l_1\sigma q_2\\
&\quad+d_2d_1\sigma\cdot l_1S_2^E(q_2\beta_{V_2}\frac{\xi}{\sigma}+\sigma\beta_{I_2}\frac{\alpha}{w_2+\gamma+\mu}+\beta_{E_2}q_2)-l_1d_1\cdot d_2d_1q_2\sigma\\
&=d_2(q_2\sigma+d_1q_2)\cdot l_1S_2^E(q_2\beta_{V_2}\frac{\xi}{\sigma}+\sigma\beta_{I_2}\frac{\alpha}{w_2+\gamma+\mu})+d_2q_2\sigma\cdot l_1\sigma q_2
\end{aligned}
$$

$$
\begin{aligned}
&+ d_2d_1\sigma \cdot l_1 \cdot \frac{d_1}{\beta_{V_2}\frac{\xi}{\sigma} + \beta_{I_2}\frac{\alpha}{w_2+\gamma+\mu} + \beta_{E_2}} q_2(\beta_{V_2}\frac{\xi}{\sigma} + \frac{\sigma}{q_2}\beta_{I_2}\frac{\alpha}{w_2+\gamma+\mu} + \beta_{E_2}) \\
&- l_1d_1 \cdot d_2d_1q_2\sigma \\
\geq& d_2(q_2\sigma + d_1q_2) \cdot l_1 S_2^E (q_2\beta_{V_2}\frac{\xi}{\sigma} + \sigma\beta_{I_2}\frac{\alpha}{w_2+\gamma+\mu}) + d_2q_2\sigma \cdot l_1\sigma q_2 \\
&+ d_2d_1\sigma \cdot l_1 \cdot d_1q_2 - l_1d_1 \cdot d_2d_1q_2\sigma \\
=& d_2(q_2\sigma + d_1q_2) \cdot l_1 S_2^E (q_2\beta_{V_2}\frac{\xi}{\sigma} + \sigma\beta_{I_2}\frac{\alpha}{w_2+\gamma+\mu}) + d_2q_2\sigma \cdot l_1\sigma q_2 \\
>& 0;
\end{aligned}
$$

(ii)if $\sigma \leq q_2$,

$$
\begin{aligned}
m_2 =& d_2(q_2\sigma + d_1q_2 + d_1\sigma) \cdot l_1 S_2^E (q_2\beta_{V_2}\frac{\xi}{\sigma} + \sigma\beta_{I_2}\frac{\alpha}{w_2+\gamma+\mu}) \\
&+ l_1\beta_{E_2}S_2^E \cdot d_2d_1q_2\sigma + d_2q_2\sigma \cdot l_1\sigma q_2 - l_1d_1 \cdot d_2d_1q_2\sigma \\
=& d_2(q_2\sigma + d_1\sigma) \cdot l_1 S_2^E (q_2\beta_{V_2}\frac{\xi}{\sigma} + \sigma\beta_{I_2}\frac{\alpha}{w_2+\gamma+\mu}) + d_2q_2\sigma \cdot l_1\sigma q_2 \\
&+ d_2d_1q_2 \cdot l_1 S_2^E (q_2\beta_{V_2}\frac{\xi}{\sigma} + \sigma\beta_{I_2}\frac{\alpha}{w_2+\gamma+\mu} + \beta_{E_2}\sigma) - l_1d_1 \cdot d_2d_1q_2\sigma \\
=& d_2(q_2\sigma + d_1\sigma) \cdot l_1 S_2^E (q_2\beta_{V_2}\frac{\xi}{\sigma} + \sigma\beta_{I_2}\frac{\alpha}{w_2+\gamma+\mu}) + d_2q_2\sigma \cdot l_1\sigma q_2 \\
&+ d_2d_1q_2l_1 \frac{d_1}{\beta_{V_2}\frac{\xi}{\sigma} + \beta_{I_2}\frac{\alpha}{w_2+\gamma+\mu} + \beta_{E_2}} \sigma(\frac{q_2}{\sigma}\beta_{V_2}\frac{\xi}{\sigma} + \beta_{I_2}\frac{\alpha}{w_2+\gamma+\mu} + \beta_{E_2}) \\
&- l_1d_1 \cdot d_2d_1q_2\sigma \\
\geq& d_2(q_2\sigma + d_1\sigma) \cdot l_1 S_2^E (q_2\beta_{V_2}\frac{\xi}{\sigma} + \sigma\beta_{I_2}\frac{\alpha}{w_2+\gamma+\mu}) + d_2q_2\sigma \cdot l_1\sigma q_2 \\
&+ d_2d_1q_2 \cdot l_1 \cdot d_1\sigma - l_1d_1 \cdot d_2d_1q_2\sigma \\
=& d_2(q_2\sigma + d_1\sigma) \cdot l_1 S_2^E (q_2\beta_{V_2}\frac{\xi}{\sigma} + \sigma\beta_{I_2}\frac{\alpha}{w_2+\gamma+\mu}) + d_2q_2\sigma \cdot l_1\sigma q_2 \\
>& 0,
\end{aligned}
$$

and it is concluded that in either case m_2 is greater than zero.

In brief, $m_i > 0$ hold for $i = 1, 2, 3, 4, 5, 6$, and the local asymptotic stability of x_2^E establishes.

Appendix B: Global stability of the endemic equilibrium in the entire system

We provide details of the proof that when $\mathcal{R}_{02} > 1$, the endemic equilibrium

$$x^{EE} = (S_1^{EE}, E_1^{EE}, I_1^{EE}, V_1^{EE}, S_2^E, E_2^E, I_2^E, V_2^E)$$

for the two-patch system is globally asymptotically stable. From Theorem 3.2 we know that the endemic equilibrium $(S_2^E, E_2^E, I_2^E, V_2^E)$ of the single-patch subsystem (2.2) is globally asymptotically stable in patch 2 when $\mathcal{R}_{02} > 1$. Thus

$\lim_{t\to\infty} S_2(t) = S_2^E$, and $\lim_{t\to\infty} E_2(t) = E_2^E$. Hence, it suffices to consider the limiting system of (2.1):

$$\begin{aligned}
\frac{dS_1}{dt} &= \Lambda_1 - \beta_{E_1} S_1 E_1 - \beta_{I_1} S_1 I_1 - \beta_{V_1} S_1 V_1 - \mu S_1 + a_2 S_2^E, \\
\frac{dE_1}{dt} &= \beta_{E_1} S_1 E_1 + \beta_{I_1} S_1 I_1 + \beta_{V_1} S_1 V_1 - (\alpha+\mu) E_1 + b_2 E_2^E, \\
\frac{dI_1}{dt} &= \alpha E_1 - (w_1 + \gamma + \mu) I_1, \\
\frac{dV_1}{dt} &= \xi E_1 - \sigma V_1,
\end{aligned} \tag{6.1}$$

and show that its positive equilibrium $(S_1^{EE}, E_1^{EE}, I_1^{EE}, V_1^{EE})$ is globally asymptotically stable in patch 1. We have

$$\begin{aligned}
&\Lambda_1 - \beta_{E_1} S_1^{EE} E_1^{EE} - \beta_{I_1} S_1^{EE} I_1^{EE} - \beta_{V_1} S_1^{EE} V_1^{EE} - \mu S_1^{EE} + a_2 S_2^E = 0, \\
&\beta_{E_1} S_1^{EE} E_1^{EE} + \beta_{I_1} S_1^{EE} I_1^{EE} + \beta_{V_1} S_1^{EE} V_1^{EE} - (\alpha+\mu) E_1^{EE} + b_2 E_2^E = 0, \\
&\alpha E_1^{EE} - (w_1+\gamma+\mu) I_1^{EE} = 0, \\
&\xi E_1^{EE} - \sigma V_1^{EE} = 0.
\end{aligned} \tag{6.2}$$

We construct a Lyapunov function

$$\begin{aligned}
\mathcal{L} = &\int_{S_1^{EE}}^{S_1} \frac{u - S_1^{EE}}{u} du + \int_{E_1^{EE}}^{E_1} \frac{u - E_1^{EE}}{u} du + \frac{\beta_{I_1} S_1^{EE} I_1^{EE}}{\alpha E_1^{EE}} \int_{I_1^{EE}}^{I_1} \frac{u - I_1^{EE}}{u} du \\
&+ \frac{\beta_{V_1} S_1^{EE} V_1^{EE}}{\xi E_1^{EE}} \int_{V_1^{EE}}^{V_1} \frac{u - V_1^{EE}}{u} du.
\end{aligned}$$

The derivative of $\mathcal{L}$ along the solution of (6.1) is:

$$\begin{aligned}
\mathcal{L}' =&(1 - \frac{S_1^{EE}}{S_1}) S_1' + (1 - \frac{E_1^{EE}}{E_1}) E_1' + \frac{\beta_{I_1} S_1^{EE} I_1^{EE}}{\alpha E_1^{EE}} (1 - \frac{I_1^{EE}}{I_1}) I_1' \\
&+ \frac{\beta_{V_1} S_1^{EE} V_1^{EE}}{\xi E_1^{EE}} (1 - \frac{V_1^{EE}}{V_1}) V_1'.
\end{aligned}$$

Thus we obtain

$$\begin{aligned}
\mathcal{L}' =&(1 - \frac{S_1^{EE}}{S_1})[\Lambda_1 - \beta_{E_1} S_1 E_1 - \beta_{I_1} S_1 I_1 - \beta_{V_1} S_1 V_1 - \mu S_1 + a_2 S_2^E \\
&- (\Lambda_1 - \beta_{E_1} S_1^{EE} E_1^{EE} - \beta_{I_1} S_1^{EE} I_1^{EE} - \beta_{V_1} S_1^{EE} V_1^{EE} - \mu S_1^{EE} + a_2 S_2^E)] \\
&(\text{marked as } k_9) \\
&+ (1 - \frac{E_1^{EE}}{E_1})\{[\beta_{E_1} S_1 E_1 + \beta_{I_1} S_1 I_1 + \beta_{V_1} S_1 V_1 - (\alpha+\mu) E_1 + b_2 E_2^E] \\
&- [\beta_{E_1} S_1^{EE} E_1^{EE} + \beta_{I_1} S_1^{EE} I_1^{EE} + \beta_{V_1} S_1^{EE} V_1^{EE} - (\alpha+\mu) E_1^{EE} + b_2 E_2^E]\} \\
&(\text{marked as } k_{10}) \\
&+ \frac{\beta_{I_1} S_1^{EE} I_1^{EE}}{\alpha E_1^{EE}} (1 - \frac{I_1^{EE}}{I_1})\{[\alpha E_1 - (w_1+\gamma+\mu) I_1] \\
&- [\alpha E_1^{EE} - (w_1+\gamma+\mu) I_1^{EE}]\}
\end{aligned}$$

$$
\begin{aligned}
&\text{(marked as } k_{11})\\
&+\frac{\beta_{V_1}S_1^{EE}V_1^{EE}}{\xi E_1^{EE}}(1-\frac{V_1^{EE}}{V_1})[\xi E_1-\sigma V_1-(\xi E_1^{EE}-\sigma V_1^{EE})]\\
&\text{(marked as } k_{12})\\
&\text{(by using the four equations of (6.2)).}
\end{aligned}
$$

Manipulating the algebra for k_9, k_{10}, k_{11} and k_{12} separately, we have

$$
\begin{aligned}
k_9 =&\mu S_1^{EE}(2-\frac{S_1}{S_1^{EE}}-\frac{S_1^{EE}}{S_1})+\beta_{E_1}(1-\frac{S_1^{EE}}{S_1})(S_1^{EE}E_1^{EE}-S_1E_1)\\
&+\beta_{I_1}(1-\frac{S_1^{EE}}{S_1})(S_1^{EE}I_1^{EE}-S_1I_1)+\beta_{V_2}(1-\frac{S_1^{EE}}{S_1})(S_1^{EE}V_1^{EE}-S_1V_1)\\
=&\mu S_1^{EE}(2-\frac{S_1}{S_1^{EE}}-\frac{S_1^{EE}}{S_1}) \quad \bigstar_1\\
&+\beta_{E_1}[S_1^{EE}E_1^{EE}-S_1E_1-\frac{(S_1^{EE})^2E_1^{EE}}{S_1}+S_1^{EE}E_1] \quad \blacktriangle_1\\
&+\beta_{I_1}[S_1^{EE}I_1^{EE}-S_1I_1-\frac{(S_1^{EE})^2I_1^{EE}}{S_1}+S_1^{EE}I_1] \quad \blacktriangle_2\\
&+\beta_{V_1}[S_1^{EE}V_1^{EE}-S_1V_1-\frac{(S_1^{EE})^2V_1^{EE}}{S_1}+S_1^{EE}V_1] \quad \blacktriangle_3,\\
k_{10} =&(\alpha+\mu)E_1^{EE}(2-\frac{E_1}{E_1^{EE}}-\frac{E_1^{EE}}{E_1})+\beta_{E_1}(1-\frac{E_1^{EE}}{E_1})(S_1E_1-S_1^{EE}E_1^{EE})\\
&+\beta_{I_1}(1-\frac{E_1^{EE}}{E_1})(S_1I_1-S_1^{EE}I_1^{EE})+\beta_{V_1}(1-\frac{E_1^{EE}}{E_1})(S_1V_1-S_1^{EE}V_1^{EE})\\
=&(\alpha+\mu)E_1^{EE}(2-\frac{E_1}{E_1^{EE}}-\frac{E_1^{EE}}{E_1}) \quad \blacktriangledown_1\\
&+\beta_{E_1}[-S_1^{EE}E_1^{EE}+S_1E_1+\frac{S_1^{EE}(E_1^{EE})^2}{E_1}-S_1E_1^{EE}] \quad \blacklozenge_1\\
&+\beta_{I_1}[-S_1^{EE}I_1^{EE}+S_1I_1-\frac{E_1^{EE}S_1I_1}{E_1}+\frac{E_1^{EE}S_1^{EE}I_1^{EE}}{E_1}] \quad \blacklozenge_2\\
&+\beta_{V_1}[-S_1^{EE}V_1^{EE}+S_1V_1-\frac{E_1^{EE}S_1V_1}{E_1}+\frac{E_1^{EE}S_1^{EE}V_1^{EE}}{E_1}] \quad \blacklozenge_3,\\
k_{11} =&\frac{\beta_{I_1}S_1^{EE}I_1^{EE}}{\alpha E_1^{EE}}(\omega_1+\gamma+\mu)I_1^{EE}(2-\frac{I_1}{I_1^{EE}}-\frac{I_1^{EE}}{I_1})\\
&+\frac{\beta_{I_1}S_1^{EE}I_1^{EE}}{\alpha E_1^{EE}}\alpha E_1^{EE}(\frac{E_1}{E_1^{EE}}-1-\frac{I_1^{EE}E_1}{I_1E_1^{EE}}+\frac{I_1^{EE}}{I_1})\\
=&\beta_{I_1}S_1^{EE}I_1^{EE}(1-\frac{I_1}{I_1^{EE}}+\frac{E_1}{E_1^{EE}}-\frac{I_1^{EE}E_1}{I_1E_1^{EE}}) \quad \divideontimes\\
&\text{(on the basis of the third equation of (6.2)),}
\end{aligned}
$$

and

$$
k_{12} =\frac{\beta_{V_1}S_1^{EE}V_1^{EE}}{\xi E_1^{EE}}\sigma V_1^{EE}(2-\frac{V_1^{EE}}{V_1}-\frac{V_1}{V_1^{EE}})
$$

$$
\begin{aligned}
&+\frac{\beta_{V_1}S_1^{EE}V_1^{EE}}{\xi E_1^{EE}}\xi E_1^{EE}(\frac{E_1}{E_1^{EE}}-1-\frac{V_1^{EE}E_1}{V_1E_1^{EE}}+\frac{V_1^{EE}}{V_1})\\
=&\beta_{V_1}S_1^{EE}V_1^{EE}(1-\frac{V_1}{V_1^{EE}}+\frac{E_1}{E_1^{EE}}-\frac{V_1^{EE}E_1}{V_1E_1^{EE}})\quad \circledast\\
&\text{(according to the fourth equation of (6.2)).}
\end{aligned}
$$

To proceed, we first decompose the term $\blacktriangledown_1$:

$$
\begin{aligned}
\blacktriangledown_1 =&(\beta_{E_1}S_1^{EE}E_1^{EE}+\beta_{I_1}S_1^{EE}I_1^{EE}+\beta_{V_1}S_1^{EE}V_1^{EE}+b_2E_2^{E})(2-\frac{E_1}{E_1^{EE}}-\frac{E_1^{EE}}{E_1})\\
&\text{(due to the second equation of (6.2))}\\
=&\beta_{E_1}S_1^{EE}E_1^{EE}(2-\frac{E_1}{E_1^{EE}}-\frac{E_1^{EE}}{E_1})\quad \blacktriangledown_{11}\\
&+\beta_{I_1}S_1^{EE}I_1^{EE}(2-\frac{E_1}{E_1^{EE}}-\frac{E_1^{EE}}{E_1})\quad \blacktriangledown_{12}\\
&+\beta_{V_1}S_1^{EE}V_1^{EE}(2-\frac{E_1}{E_1^{EE}}-\frac{E_1^{EE}}{E_1})\quad \blacktriangledown_{13}\\
&+b_2E_2^{E}(2-\frac{E_1}{E_1^{EE}}-\frac{E_1^{EE}}{E_1})\quad \blacktriangledown_{14}.
\end{aligned}
$$

Secondly, we collect the same items:

$$
\begin{aligned}
\blacktriangledown_{11}+\blacktriangle_1+\blacklozenge_1 =&\beta_{E_1}S_1^{EE}E_1^{EE}(2-\frac{E_1}{E_1^{EE}}-\frac{E_1^{EE}}{E_1}+\frac{E_1}{E_1^{EE}}-\frac{S_1^{EE}}{S_1}+\frac{E_1^{EE}}{E_1}-\frac{S_1}{S_1^{EE}})\\
=&\beta_{E_1}S_1^{EE}E_1^{EE}(2-\frac{S_1}{S_1^{EE}}-\frac{S_1^{EE}}{S_1}),\\
\blacktriangledown_{12}+\blacktriangle_2+\blacklozenge_2+\divideontimes =&\beta_{I_1}S_1^{EE}I_1^{EE}(2-\frac{E_1}{E_1^{EE}}-\frac{E_1^{EE}}{E_1}+1\\
&+\frac{E_1}{E_1^{EE}}+\frac{E_1^{EE}}{E_1}-\frac{I_1^{EE}E_1}{I_1E_1^{EE}}-\frac{S_1^{EE}}{S_1}-\frac{E_1^{EE}S_1I_1}{E_1S_1^{EE}I_1^{EE}})\\
=&\beta_{I_1}S_1^{EE}I_1^{EE}(3-\frac{I_1^{EE}E_1}{I_1E_1^{EE}}-\frac{S_1^{EE}}{S_1}-\frac{E_1^{EE}S_1I_1}{E_1S_1^{EE}I_1^{EE}}),
\end{aligned}
$$

and

$$
\begin{aligned}
\blacktriangledown_{13}+\blacktriangle_3+\blacklozenge_3+\circledast =&\beta_{V_1}S_1^{EE}V_1^{EE}(2-\frac{E_1}{E_1^{EE}}-\frac{E_1^{EE}}{E_1}+1\\
&+\frac{E_1}{E_1^{EE}}+\frac{E_1^{EE}}{E_1}-\frac{V_1^{EE}E_1}{V_1E_1^{EE}}-\frac{S_1^{EE}}{S_1}-\frac{E_1^{EE}S_1V_1}{E_1S_1^{EE}V_1^{EE}})\\
=&\beta_{V_1}S_1^{EE}V_1^{EE}(3-\frac{V_1^{EE}E_1}{V_1E_1^{EE}}-\frac{S_1^{EE}}{S_1}-\frac{E_1^{EE}S_1V_1}{E_1S_1^{EE}V_1^{EE}}).
\end{aligned}
$$

Finally, adding the three parts above to the expressions of $\bigstar_1$ and $\blacktriangledown_{14}$, we obtain

$$
\mathcal{L}' =\mu S_1^{EE}(2-\frac{S_1}{S_1^{EE}}-\frac{S_1^{EE}}{S_1})+b_2E_2^{E}(2-\frac{E_1}{E_1^{EE}}-\frac{E_1^{EE}}{E_1})
$$

$$
\begin{aligned}
&+\beta_{E_1} S_1^{EE} E_1^{EE}(2-\frac{S_1}{S_1^{EE}}-\frac{S_1^{EE}}{S_1})\\
&+\beta_{I_1} S_1^{EE} I_1^{EE}(3-\frac{I_1^{EE}E_1}{I_1E_1^{EE}}-\frac{S_1^{EE}}{S_1}-\frac{E_1^{EE}S_1I_1}{E_1S_1^{EE}I_1^{EE}})\\
&+\beta_{V_1} S_1^{EE} V_1^{EE}(3-\frac{V_1^{EE}E_1}{V_1E_1^{EE}}-\frac{S_1^{EE}}{S_1}-\frac{E_1^{EE}S_1V_1}{E_1S_1^{EE}V_1^{EE}})\\
\le& 0.
\end{aligned}
$$

Meanwhile, it is clear that

$$\{\mathcal{L}'=0\}=\{S_1=S_1^{EE}, E_1=E_1^{EE}, I_1=I_1^{EE}, V_1=V_1^{EE}\}.$$

Using LaSalle's Invariance Principle again, we obtain that (S_1^{EE}, E_1^{EE}, I_1^{EE}, V_1^{EE}) is globally asymptotically stable for the limiting system (6.1), which leads to the conclusion that the endemic equilibrium x^{EE} is globally asymptotically stable for the entire two-patch system.

References

[1] J. F. W. Chan, S. Yuan, K. H. Kok, et al., *A familial cluster of pneumonia associated with the 2019 novel coronavirus indicating person-to-person transmission: a study of a family cluster*, Lancet, 2020, 395, 514–523.

[2] P. van den Driessche and J. Watmough, *Reproduction numbers and sub-threshold endemic equilibria for compartmental models of disease transmission*, Math. Biosci., 2002, 180, 29–48.

[3] N. van Doremalen, T. Bushmaker, D. H. Morris, et al., *Aerosol and surface stability of SARS-CoV-2 as compared with SARS-CoV-1*, New Engl. J. Med., 2020, 382, 1564–1567.

[4] T. Ellerin, *The new coronavirus: What we do-and don't-know*, Harvard Health Blog, January 25, 2020. Available at https://www.health.harvard.edu/blog/the-new-coronavirus-what-we-do-and-dont-know-2020012518747

[5] N. Imai, A. Cori, I. Dorigatti, M. Baguelin, C. A. Donnelly, S. Riley, and N. M. Ferguson, *Report 3: Transmissibility of 2019-nCoV*, published online January 25, 2020. Available at https://www.imperial.ac.uk/mrc-global-infectious-disease-analysis/news--wuhan-coronavirus/

[6] K. Leung, J. Wu, D. Liu, and G. M. Leung, *First-wave COVID-19 transmissibility and severity in China outside Hubei after control measures, and second-wave scenario planning: a modelling impact assessment*, Lancet, 2020, 395, 1382–1393.

[7] Q. Li, X. Guan, P. Wu, X. Wang, L. Zhou, Y. Tong, et al., *Early transmission dynamics in Wuhan, China, of novel coronavirus-infected pneumonia*, N. Engl. J. Med., 2020, 382(13), 1199–1207.

[8] R. Li, S. Pei, B. Chen, Y. Song, T. Zhang, W. Yang, and J. Shaman, *Substantial undocumented infection facilitates the rapid dissemination of novel coronavirus (SARS-CoV2)*, Science, 2020, 368, 489–493.

[9] J. M. Read, J. R. E. Bridgen, D. A. T. Cummings, A. Ho and C. P. Jewell, *Novel coronavirus 2019-nCoV: early estimation of epidemiological parameters and epidemic predictions*, available at medRxiv. DOI: https://doi.org/10.1101/2020.01.23.20018549

[10] B. Tang, X. Wang, Q. Li, N. L. Bragazzi, S. Tang, Y. Xiao, and J. Wu, *Estimation of the Transmission Risk of 2019-nCoV and Its Implication for Public Health Interventions*, J. Clin. Med., 2020, 9(2), 462.

[11] J. Wang, *Mathematical models for COVID-19: applications, limitations, and potentials*, J. Public Health Emerg., 2020, 4, 9.

[12] J. Wu, K. Leung, and G. M. Leung, *Nowcasting and forecasting the potential domestic and international spread of the 2019-nCoV outbreak originating in Wuhan, China: a modelling study*, Lancet, 2020, 395, 689–697.

[13] C. Yang and J. Wang, *A mathematical model for the novel coronavirus epidemic in Wuhan, China*, Math. Biosci. Eng., 2020, 17(3), 2708–2724.

[14] C. Yeo, S. Kaushal and D. Yeo, *Enteric involvement of coronaviruses: is faecal-oral transmission of SARS-CoV-2 possible?* Lancet Gastroenterol., 2020, 5(4), 335–337.

[15] *Centers for Disease Control and Prevention: Coronavirus (COVID-19)*. Available at https://www.cdc.gov/coronavirus/2019-ncov

[16] *Statistical Bulletin of National Economic and Social Development of WUHAN in 2019*, 2020–03–29. Available at http://tjj.wuhan.gov.cn/tjfw/tjgb/202004/t20200429_1191417.shtml

[17] *Hubei Provincial Bureau of Statistics, Statistical Bulletin of National Economic and Social Development of Hubei Province in 2019*, 2020–03–23. Available at http://tjj.hubei.gov.cn/tjsj/tjgb/ndtjgb/qstjgb/202003/t20200323_2188487.shtml

[18] *National Bureau of Statistics*, 2019. Available at http://data.stats.gov.cn/easyquery.htm?cn=C01

[19] *The Health Commission of Hubei Province*, Available at http://wjw.hubei.gov.cn/fbjd/dtyw/index_16.shtml

[20] *National Health Commission of the People's Republic of China*, Data of Confirmed Cases on COVID-19, 2020. Available at http://www.nhc.gov.cn/xcs/xxgzbd/gzbd_index.shtml